Vol 28 No. 1 Jan - Mar 2012 ISSN 0970-5953

PHYSICS EDUCATION

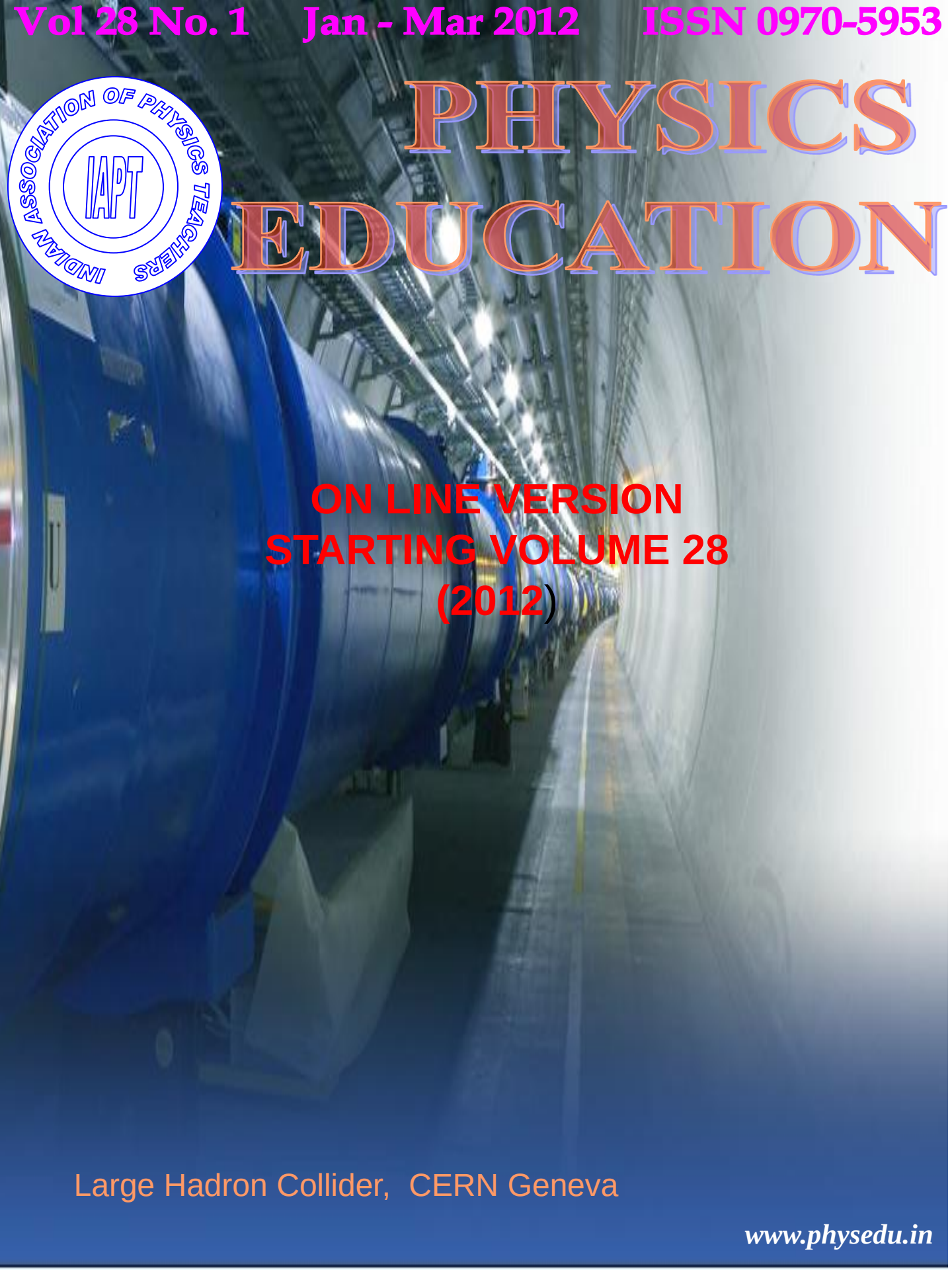

ON LINE VERSION
STARTING VOLUME 28
(2012)

Large Hadron Collider, CERN Geneva

www.physedu.in

Volume 28, Number 1

In this Issue

EDITORIAL

(*Submitted* 01 – 03 - 2012)

Physics Education begins an era of online publication with this issue. With this step we expect the journal to enlarge its reach among the Physics Community in our colleges and Universities more directly in a participatory mode. At present it will retain almost the same format as well as the frequency of publication as in the preceding volumes. In order to emphasize the continuity, we call this issue as the first number of Volume 28. Readers may be aware that Volume 27, Issue 4 carried the date line Oct-Dec 2010. The Physics Education remained suspended during the year 2011 and the interval was used making the transition from print format to online format. We envisage online process for paper submission to the journal, peer review, editorial process and the subsequent publication. We have made the access to the journal completely free, so that there is a wider readership for the contributions of our authors. Please ask your librarian to add www.physedu.in to the List of online journals for ready access in your College or University.

We expect that the teachers will make use of the computer as an important tool for pedagogy. There are many course-wares available at many sites. Quite many resources are available to freely download and adopt them to our needs. There is some trend that authors prefer to publish e-books and make them free for any genuine user. Physics Education readers, will bring them to the notice of all of us to benefit.

The journal's utility depends directly on the quality of its content and it is here that I must appeal to you. I invite you to use this medium to share with your colleagues all your successful ventures in Physics pedagogy at both under-graduate and post-graduate levels. Taking advantage of this being an online venture, we have also enlarged the team of Editors to run the journal and thus we expect increased diversity in the content of the journal. It is only natural that other developments that are possible in the e-format will also take place soon. Pramod S Joag as the Chief Editor and R Ramachandran as the Consulting Editor look forward to an exciting future for Physics Education, as we welcome the new team of Editors to join us in this experiment. We also look forward to wise counsel from the eminent members of the Advisory Board. Readers will share with us, we hope their feedback their comments on the articles published as well as make any suggestions for us to adopt in making the journal more useful for all of us.

Pramod S Joag
Chief Editor, Physics Education
R Ramachandran
Consulting Editor, Physics Education

Filament temperature of low power incandescent lamps: Stefan-Boltzmann law

Imtiaz Ahmad, Sidra Khalid and Ehsan E. Khawaja
School of Science and Technology, University of Management and Technology,
C-II Johar Town, Lahore 54770, Pakistan
(*Submitted* February 2009)

Abstract

An undergraduate experiment using commercially available low power incandescent lamps was performed. The results obtained, for higher temperature of the filament (say above 1000 K), were compared with those calculated using a simple model, based on transfer of electric power predominantly into Planck's radiation channel through Stefan-Boltzmann law. The agreement between the results and the theory was quite satisfactory. Measurement of filament temperature to confirm theoretical results, included in the present work, is expected to give a student more confidence in the theory.

1. Introduction

There are a number of methods for estimating the temperature of the filament of incandescent lamps [1-5]. These methods are for example (i) the power law between the resistance, R, and temperature, T, of tungsten filament, (ii) the transfer of the input electric power predominantly into Planck's radiative channel through Stefan's law, (iii) exploits the fact that the lifetime of the lamp filament is mostly governed by the rate of thermal evaporation of the metal, (iv) analyses of the radiation emitted by the filament at two well defined wavelengths and (v) study of hysteresis in the current-voltage characteristics in filament lamp.

Incandescent light bulbs, in addition to providing illumination, are useful in the context of teaching physics [2,4]. In the present work two sets of measurement were made on commercially available low power lamps. These measurements were made on lamp filament: (a) resistance (R) – voltage (V) and (b) temperature (T) – voltage. An attempt is made to relate these results to those derived on the basis of transfer of the electrical power predominantly into Planck's radiation channel through Stefan-Boltzmann law.

2. Experimental

In the present work three 12-V operated low power (rated at 10-W, 25-W and 35-W) commercial lamps were studied. Current (I) – voltage measurements were performed using a variable dc power supply. Multimeters were used to measure the voltage across the filament and current in the series circuit. The resistance of the filament was obtained using R = V/I. The temperature of the filament at different voltage was measured using a Minolta-Land infrared optical pyrometer Cyclops 52. The temperatures were measured for different setting of emissivity, such as 0.3, 0.35, and 0.4. The average value of the emissivity for tungsten filament lamp is close to 0.35 [2]. Therefore, in this work e = 0.35 was used. However, the measured temperature values were larger (by less than 2.5%) for e = 0.3 and smaller (by less than 1.5%) for e = 0.4 when both compared with those obtained for e = 0.35.

3. Modeling

At a given voltage across the filament of the lamp, a steady state is reached when the current (I) passing through the filament is

stabilized. In the steady state it is expected that the electrical power input to the lamp is equal to the power lost by the filament through conductive, convective, and radiative processes, such that [2]

$$V^2 / R = K (T - T_0) + e \sigma A_s (T^4 - T_0^4) \qquad (1)$$

where K represents conductive and convective properties of the system. T and T_0 are the temperatures in Kelvin for the filament and the ambient, respectively. e and A_s are the emissivity and surface area of the filament, respectively, and σ is the Stefan-Boltzmann constant.

For higher temperature of the filament (say above 1000 K), it is reasonable to assume that $T^4 >> T_0^4$. Moreover, for low power bulbs [2], such as those used in the present work, the literature indicates that convection and conduction losses are negligible. Hence equation (1) may be rewritten as

$$V^2 = e \sigma A_s T^4 R \qquad (2)$$

Metal resistance increases with temperature. The temperature of tungsten in the range 300 K to 3655 K, can be given in terms of its resistivity (ρ) by the empirical relation, valid in SI units [7]

$$T = 3.05 \times 10^8 \rho^{0.83} \qquad (3)$$

A power relation similar to this is also given in Ref. [3, 8]. Equation (3) may be written as

$$T = 3.05 \times 10^8 [(A_c R) / L]^{0.83} \qquad (4)$$

where A_c and L are the area of cross section and length, respectively, of the filament wire. Substituting this value of T in equation (2), we have

$$V^2 = e \sigma A_s R \{3.05 \times 10^8 [(A_c R) / L]^{0.83}\}^4 \qquad (5)$$

Also, $A_s = 2\pi rL$ and $A_c = \pi r^2$, where r is the radius of the filament wire. The value of e = 0.35 (following Clauss et al [2]) and $\sigma = 5.67 \times 10^{-8}$ Wm^{-2} K^{-4} were used in the present work. Thus, equation (5) becomes

$$R = B_1 V^p \qquad (6)$$

where,

$$B_1 = 2.1 \times 10^{-7} L^{0.54} r^{-1.8} \qquad (6a)$$

and

$$p = 0.46 \qquad (6b)$$

The resistance of the filament at room temperature (R_{RT}) is given by

$$R_{RT} = \rho_{RT} (L / \pi r^2) \qquad (6c)$$

where ρ_{RT} is the resistivity of tungsten at room temperature, given by equation (3).

Similarly by eliminating R from equations (2) and (5), we obtain an expression relating T with V, such as

$$T = B_2 V^q \qquad (7)$$

Where

$$B_2 = 2.4 \times 10^3 r^{0.19} L^{-0.38} \qquad (7a)$$

and

$$q = 0.38 \qquad (7b)$$

In the present work we have measured R and T both as functions of V.

4. Results and discussion

Three unbranded 12–V operated low power lamps were acquired from the local market. The cost of each of the three lamps is given in table 1. The values of the resistance (R_{RT}) of the filaments of the three lamps measured at room temperature are listed in table 1. These were measured using Wheatstone bridge method.

Rated power of lamp (W)	Cost ($)	*R_{RT} (Ω)	**Measured B_1 (Ω-$V^{-0.46}$)	**Exponent p	***Δp	Length of filament wire L (cm)	Radius of the filament wire r (μm)
10	0.08	1.8	5.8	0.45	2%	9.5	32
25	0.15	0.68	2.0	0.49	7%	17	69
35	0.50	0.50	1.7	0.48	5%	12	68

Table 1 Various parameters of the lamp filaments: Study of R as a function of V.
* R_{RT} is the filament resistance at room temperature, measured by Wheatstone bridge method.
** Determined from plot of *log* R versus *log* V (figure 2).
*** $\Delta p = \{ [I0.46 - p I] / 0.46 \} \times 100$

The results of the measurement of R as a function of V for the lamps are shown in figure 1. Using the data of figure 1, log R versus log V is plotted in figure 2.

The dots in figure 2 represent experimental results while straight line is the result of computer generated least square fit to the data. The slope and y-intercept of a straight line (figure 2) give, respectively, the power p of V and log B_1 (see equation 6). The values of the exponent p and B_1 thus obtained from figure 2, are listed in table 1. These values of p are close (within 7%) to the theoretical value of p = 0.46 (equation 6b). For the measured values of B_1 and R_{RT} (table 1), and the value of ρ_{RT} obtained from equation (3), equations (6a) and (6c) could be solved simultaneously to obtain the values of L (length) and r (radius) of the filament wire. These parameters for the three lamps are listed in table 1. The results of the measurement of filament temperature, T, as a function of V for the three lamps may be used to provide data of log T versus log V plotted in figure 3. The dots in figure 3 represent experimental results while straight line is the result of computer generated least square fit to the data. The slope and y-intercept of a straight line give, respectively, the power q of V and log B_2 (see equation 7). The values of the exponent q and B_2 thus obtained from figure 3, are listed in table 2. These values of q are within 16% to the theoretical value of q = 0.38 (equation 7b). Using the values of the parameters L and r (table 1), B_2 were calculated from equation (7a). These are also listed in table 2. The difference between the calculated and measured values of B_2 was found to be as large as 22% (see table 2). Simple model used in the present work was based on some assumptions which may introduce errors. The filament was assumed to be uniform cylinder of cross-sectional area A_c and length L. The assumption of uniformity neglects the possibility that a real filament has thin regions due to mechanical processing needed to form the coil as well as evaporation during using which effectively limits the useful lifetime of the lamp [2]. The assumption of a cylinder instead of a coil will overestimate the effective radiating area [6], since the regions on the inside of a coil radiate back and forth, trapping some of the energy and resulting in higher filament temperatures than would be

obtained with a straight cylinder. This is more obvious in the 25-W lamp since measured temperature (at given voltage) is larger than that calculated (Table 2). On the contrary the measured temperatures were smaller than those calculated for 10–W and 35–W lamps. On examining lamp filaments under a magnifying glass it was observed that spacing between the turns was much smaller in case of 25–W lamp as compared with the corresponding for the 10–W or 35–W lamps. The volumetric thermal expansion of the filament only provides a correction of less than 2 % [5]. Chemical impurities in the tungsten wire may be another factor that have contributions to the observed differences in the measured and calculated values of various parameters (tables 1 and 2).

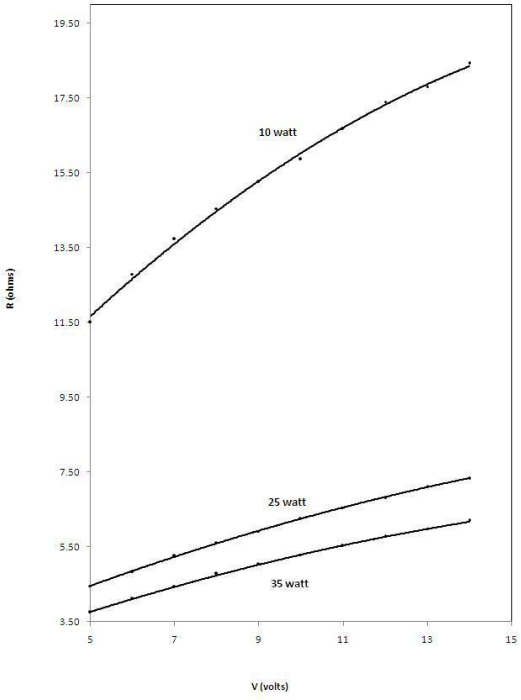

Figure 1 Resistance versus voltage curves obtained with 10 W, 25 W and 35 W incandescent lamps.

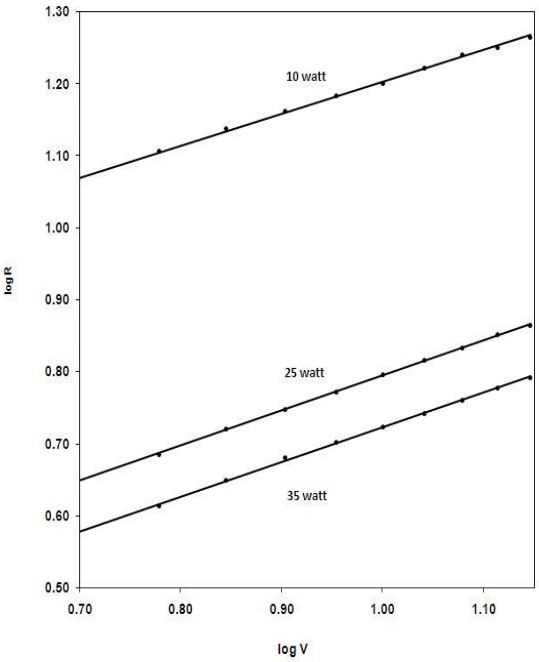

Figure 2 Log R versus log V curves (based on the data of figure 1). The dots represent experimental data and the straight line represents least square fit to the data generated by a computer.

It was reported [5] that emissivity of the filament depends on its temperature. When emissivity of the filament is assumed to be independent of temperature, then we have electric power is proportional to T^4, and this would give

R proportional to V^p, where p = 0.46(Eq. 6) and T proportional to V^q, where q = 0.38 (Eq. 7)

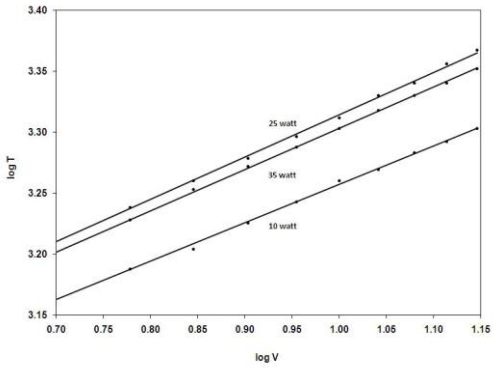

Figure 3 Log T versus log V curves (based on the data of figure 3). The dots represent experimental data and the straight line represents least square fit to the data generated by a computer

Rated power of lamp (W)	*Exponent q	**Δq	*Measured B_2 (Ω-K-$V^{-0.38}$)	***Calculated B_2 (Ω-K-$V^{-0.38}$)	****ΔB_2
10	0.32	16%	8.7×10^2	8.2×10^2	6%
25	0.35	8%	9.3×10^2	7.6×10^2	22%
35	0.35	8%	9.1×10^2	8.7×10^2	5%

Table 2 Various parameters of the lamp filaments: Study of T as a function of V

* Determined from plot of *log* T versus *log* V (figure 4).

**Δq = { [I0.38 – q I] / 0.38 } × 100.

*** Calculated from equation (7a) using the values of L and r from Table 1.

**** ΔB_2 = I[(Calculated B_2 – Measured B_2) / Calculated B_2] I× 100.

If we take emissivity to be proportional to T (as in Ref. [5]), then we have electric power proportional to T^5, and this would give

R proportional to $V^{0.39}$

and T proportional to $V^{0.32}$

The average value of the exponent, p, is 0.47 (table 1) and this is closer to 0.46 (for emissivity being independent of T) rather than 0.39 (the value for emissivity being dependent on T). Following above this value of p suggests that the emissivity may not depend significantly on temperature. The average value of exponent q = 0.34 (T versus V^q, table 2). This suggests that the emissivity may depend on temperature, though not necessarily a linear dependence. However, the results of R versus V are less affected as compared with the results of T versus V, by the uncertainties (outlined above) involved in this work. Therefore, we may suggest that emissivity of the filament is nearly independent of temperature in the present case. It was concluded in Ref. [5] that for tungsten filament whose surface is oxidized its emissivity is independent of temperature. May be this is the case in the present work.

5. Conclusions

An experiment using low-power

incandescent lamps for the verification of Stefan-Boltzmann law was carried out. Two separate sets of measurements were made on the lamps. These included filament resistance versus applied voltage and filament temperature versus applied voltage. The results were compared with those calculated using a simple model. Overall, satisfactory results were obtained.

Such an experiment may be a good addition in student laboratory. Measurement of filament temperature to confirm theoretical results is expected to give a student some confidence in theory. Most of the equipment used is readily available in the laboratory or can be easily acquired from a local market. Some effort is needed to acquire a pyrometer for measuring the filament temperature.

Acknowledgement

The support provided by the University of Management and Technology is acknowledged.

References

[1] Agrawal D C and Menon V J 1998 *Phys. Educ.* **33** 55
[2] Clauss D A, Ralich R M and Ramsier R D 2001 *Eur. J. Phys.* **22** 385
[3] Zanetti V. 1985 *Am. J. Phys.* **53** 546
[4] Edmonds I R 1968 *Am. J. Phys.* **36** 845
[5] Prasad B S N and Mascarenhas R 1978 *Am. J. Phys.* **46** 420
[6] Leff H S January 1990 *The Phys. Teacher* **28** 30
[7] 36th International Olympaid, Salamanca , Spain 2005 Planck's constant in the light of an incandescent lamp, webpage www.jyu.fi/tdk/kastdk/olympiads/2005/Exp.pdf.
[8] Denardo B 2002 *The Phys. Teacher* **40** 101

S. Chandrasekhar : White Dwarfs, H^- ion,.., Black holes, Gravitational waves

Patrick Das Gupta
*Department of Physics and Astrophysics, University of Delhi, Delhi - 110 007 (India)**

This is a concise review of S. Chandrasekhar's research contributions to astrophysics, ranging from his early studies on white dwarfs using relativistic quantum statistics to topics as diverse as dynamical friction, negative hydrogen ion, fluid dynamical instabilities, black holes and gravitational waves. The exposition is based on simple physical explanations in the context of observational astronomy, addressed primarily to the undergraduate students. Black holes and their role as central engines of active, compact, high energy sources have been discussed in some details.

I INTRODUCTION

The impactful research journey of Subrahmanyan Chandrasekhar began on July 31, 1930, from Bombay port on a ship. The 19 year old Chandra was on his way to England for higher studies. Armed with his understanding of Fowler′s work on white dwarfs [1], Chandra was immersed in the mathematical equations describing these dense objects, during that voyage. He had realized that Fowler's theory needed modification, since for sufficiently massive white dwarfs, particle number densities could be so high that a large fraction of electrons would be occupying very high energy levels, moving with relativistic velocities.

At this point, a quick summary of stellar evolution theory is in store. In main sequence stars (like Sun), nuclear fusion of hydrogen to helium supplies the required thermal energy to stall gravitational contraction of a star, enabling it to attain a quasi-hydrostatic equilibrium. As the star advances in age, a further sequence of nuclear fusion reactions gets activated in its core - helium burning to carbon and oxygen, carbon burning to sodium and magnesium and so on, if the star is massive enough, till the formation of iron-rich core. Iron nucleus being the most stable one, subsequent nuclear burning cease to take place. As the core cools, it collapses under its own weight, till the electron density becomes so high that electron degeneracy pressure prevents further contraction.

Degeneracy pressure is a consequence of quantum statistics in extremely dense matter. Pauli exclusion principle (PEP) states that no two identical fermions can have the same state. Electrons, protons, neutrons, neutrinos, etc., being spin half particles, are fermions. According to PEP, in a gravitationally bound system like the iron-rich core of an evolved star, all the electrons cannot occupy the lowest energy level (unlike, what happens to identical bosons in Bose-Einstein condensates, e.g. He-4 superfluid). So, the energy levels are filled up with two electrons (one with spin up state and the other with spin down) per orbital, as demanded by the PEP. Hence, more the density of electrons, higher is the energy level that gets to be occupied.

Gravitational shrinking of such a dense core leads to an increase in electron density, thereby facing a resistance since the contraction implies putting electrons at higher energy levels. Therefore, in such a degenerate system, gravitational collapse instead of lowering the energy of the star tends to increase it. The resulting pressure against shrinking, arising out of PEP in such electron-rich dense matter is called electron degeneracy pressure (EDP). A white dwarf is a star that is in hydrostatic equilibrium not because of thermal pressure but due to the EDP that counteracts gravitational contraction. Fowler had assumed that electrons are moving non-relativistically inside the core and had shown that the EDP of a white dwarf is proportional to $\rho^{5/3}$, where ρ is the density of the core[1].

II CHANDRASEKHAR LIMIT AND COMPACT OBJECTS

In his investigations, Chandra incorporated special relativity in the analysis of white dwarfs, and found that the EDP is proportional to $\rho^{4/3}$ instead, demonstrating that the relativistic degeneracy pressure does not increase as rapidly as in Fowler's case. Performing an accurate study of the relativistic problem of a dense star ruled by a polytropic equation of state, in which gravity is countered by the EDP, he arrived at the celebrated Chandrasekhar mass limit [2],

$$M_{Ch} = \frac{0.2}{(m_p \mu_e)^2} \left(\frac{\hbar c}{G}\right)^{3/2} \quad , \tag{1}$$

where $\hbar$, G, c, m_p and μ_e are the reduced Planck′s constant, Newton′s gravitational constant, speed of light, mass of a proton and mean molecular weight per electron, respectively. It is remarkable that such a significant result concerning stars should be expressible in terms of fundamental quantities (except for μ_e). In white dwarfs, the value of μ_e is about 2, so that from eq.(1) one finds the limit to be $M_{Ch} \approx 1.4\ M_\odot$, where $M_\odot = 2 \times 10^{30}$ kg is the Sun′s mass.

Chandra was unaware initially that Anderson in 1929 and Stoner in 1930 had independently applied special relativity to obtain mass limits for a degenerate, dense star of uniform density without taking into account the condition of hydrostatic equilibrium [3,4,7]. Fowler pointed

this out to him when Chandra reached Cambridge, and he added these references to his papers on relativistic degeneracy in white dwarf stars [5]. Landau too had arrived at a mass limit independently in 1931, which appeared in print one year later [6].

The Chandrasekhar mass limit implies that no white dwarf with mass greater than this limit can hold out against gravitational collapse. So far, all the white dwarfs discovered (e.g. Sirius B, the companion star to Sirius) in the cosmos, have mass less than M_{Ch}. For masses beyond this limit, two prescient ideas were put forward independently, that played important roles later - one of Landau [6], before the discovery of neutrons by Chadwick in 1932 and the other by Baade and Zwicky [8,9], after the discovery. Landau had speculated that for stellar cores whose mass exceeded M_{Ch}, the density would become so large due to shrinking that the atomic nuclei in the core would come in contact with each other - the whole core turning into a giant nucleus [6]. Baade and Zwicky, while attributing the origin of cosmic rays to stellar explosions called supernovae, correctly identified the energy liberated due to sudden decrease in the gravitational potential energy (as the core collapses rapidly to form a neutron star of radius $\sim$ 10 km) as the one that powers supernova explosion [8,9]. A core with mass M_c, shrinking from a large size to a radius R_c, has to give up an energy,

$$E_{exp} \sim \frac{GM_c^2}{R_c} \quad , \tag{2}$$

since its gravitational potential energy decreases to $\sim -E_{exp}$. For a 1.4 $M_\odot$ core collapsing to form a neutron star of radius $R_c \approx 10$ km, the energy E_{exp} available for explosion is as high as $\sim 10^{53}$ ergs.

Why does the core become neutron-rich? As the core shrinks, its density rises till it reaches nucleonic values $\sim 10^{12}$ - 10^{14} gm/cm^3, when protons in the core transform into neutrons by capturing electrons and emitting neutrinos [10]. Neutrinos, being weakly interacting particles, escape from the core. While in the neutron-rich core, the neutron degeneracy pressure (arising from PEP, as neutrons too are spin half particles) prevents further gravitational contraction, resulting in the formation of a neutron star.

With the detection of periodic emission of radio-pulses from a source by Jocelyn Bell and Anthony Hewish in 1967, existence of neutron stars as pulsars was established. Pulsars are rapidly spinning neutron stars with rotation period ranging from about few milli-seconds to few seconds. The observed pulses are due to electromagnetic radiation from accelerated charge particles moving along strong magnetic field lines inclined with respect to the rotation axis (The polar magnetic field strengths vary from $\sim 10^{10}$ to $\sim 10^{14}$ gauss). Recently, a milli-second pulsar was found to have a mass of ≈ 2 $M_\odot$, determined using a general relativistic effect called Shapiro delay in which radiation grazing past a compact, massive object, arrives at the observer with a time lag because of the strongly curved space-time geometry it encounters near the massive star [11].

As long as the core is lighter than about $2-3$ $M_\odot$, it can survive as a neutron star (The mass limit in this case is uncertain as it depends crucially on the equation of state for nuclear matter which, for such huge densities existing inside neutron stars, is unknown [11,12]). The released neutrinos, after travelling long distances, eventually lose their energy to the stellar envelope, causing the latter to be blown apart, giving rise to a Type II supernova. Measurements concerning detected neutrinos from the supernova SN 1987A indicate that these ultra-light, weakly interacting particles carry away 99% of the gravitational binding energy released from the collapsing core, lending credence to the neutrino driven explosion models [10].

The observed masses for neutron stars do not appear to exceed ~ 3 $M_\odot$ [11,12], suggesting that a massive star whose core is heaver than this limit, would certainly collapse to form a black hole. The long duration gamma ray burst sources that exhibit prompt gamma emissions with photons having energy predominantly in 0.1 - 1 MeV range, and lasting for about 2 - 1000 s are likely to be collapsing massive cores [13]. Eddington had found the idea of a star shrinking gravitationally to a point absurd [14]. Three decades later, Penrose and Hawking, employing Raychaudhuri equation, proved the remarkable singularity theorems, according to which gravitational collapse of normal matter generically lead to formation of point singularities, namely, the black holes [15–17].

III DYNAMICAL FRICTION

Chandra played a significant role in the research area of stellar dynamics from 1939 to 1944 that culminated in the publication of his celebrated papers on dynamical friction[18,19]. Cosmos is filled with gravitationally bound systems of massive objects like globular clusters, galaxies, clusters of galaxies, etc. Objects that make up these bound systems, apart from moving in gravitational potential wells, also suffer two-body gravitational encounters, resulting in exchange of energy and momentum. It was Chandra who showed for the first time that a massive body in motion, surrounded by a swarm of other less massive objects, suffers deceleration that is proportional to its mass [18].

Dynamical friction arises out of cumulative gravitational encounters that the massive body experiences due to the presence of other objects in the background. The physical origin of dynamical friction can be intuitively understood by going to the reference frame in which the body is at rest. In this frame, the swarm of background objects while moving past the massive body get grav-

itationally focused behind the body, forming a wake of higher mass density. Now, switching back to the frame in which the massive body is moving, we find that the mass density of the wake behind is greater than the density ahead. Consequently, because of a greater gravitational pull from behind, the massive body suffers a gravitational drag force whose magnitude is proportional to the square of its mass and inversely proportional to the square of its speed [20,21].

Observational consequences of dynamical friction include sinking of globular clusters towards the central regions of galaxies and galactic cannibalism in which the orbit of a satellite galaxy decays, leading eventually to its merger with the bigger galaxy [21,22].

IV NEGATIVE HYDROGEN ION

Around the same time, Chandra was also involved with the quantum theory of negative hydrogen ion. Can a proton capture two electrons to form a charged bound state? How is it relevant to astrophysics? The first issue had been settled by Bethe in 1929 who showed that quantum mechanics indeed predicts formation of H^- ions [23]. As to the second question, it has been found over the years that H^- is a weakly bound system with a binding energy of ≈ 0.75 eV. Since it takes only about 0.75 eV to knock off the extra electron from H^-, its life-time under terrestrial conditions is small but in thin and tenuous plasma where the collision frequency is low, one expects negative hydrogen ions to survive for longer duration.

Early on, Wildt had foreseen that because of the presence of hydrogen atoms and electrons, in large numbers, in the upper atmosphere of Sun, H^- would form. He had also realized that photo-detachment of H^- would contribute greatly to solar opacity, since radiation from Sun would be attenuated as they photo-ionize H^- ions on their way out[24–26].

At this juncture, Chandra and his collaborators played an important role in calculating H^- photo-absorption matrix element, so crucial for estimating the quantum probability (and, therefore, the cross-section) of photo-ionization of H^- [27–33]. The opacity or the optical depth is proportional to the photo-absorption cross-section σ as well as n, the number density of H^-. This is because, the number of photo-ionizations per photon per unit time is $c\ n\ \sigma$, so that the mean free path length for photons is simply,

$$l = \frac{1}{n\ \sigma} \quad .$$

The optical depth essentially is the ratio of the geometrical path length traversed by the radiation to mean free path length l (i.e., it is the number of absorptions suffered by the photons on an average).

The negative hydrogen ion has only the ground state as a bound state, with no singly excited states. As a result, photons with energy above 0.75 eV, executing random walks out of Sun due to multiple scatterings, would be absorbed by H^- ions after detaching their extra electrons to the continuum. This is the dominant cause for solar opacity in the infra-red to visible range of the electromagnetic spectrum.

In 1943, Chandrasekhar and Krogdahl drew attention to the fact that dominant contribution to this matrix element comes from the wavefunction at large distances (several times the Bohr radius), and therefore an accurate knowledge of electronic wavefunction of H^- was required [27].

Chandra and his collaborators made seminal contributions towards calculating the continuous absorption coefficient κ_λ of H^- as a function of the photon wavelength λ, incorporating dipole-length and dipole-velocity formulae, that provided a solid theoretical foundation for the characteristic κ_λ - λ plot which exhibits a rise in the range 4000 to 9000 angstroms and then drops to a minimum at 16000 angstroms, with a subsequent rise [34].

The charged hydrogen ion has also played an important role in cyclotrons and particle accelerators [35]. The advantages in making use of H^- arise out of the possibility of accelerating them by applying electric fields and obtaining hot neutral beams in Tokamaks (like in ITER)[36]. This is because of the relative ease in detaching its extra electron when H^- ion is present in the gas cells.

V MAGNETOHYDRODYNAMICS

Astrophysical entities are usually permeated with magnetic fields, be it planets like earth, Jupiter, etc., Sun, sunspots, stars, flares, spiral arms of Milky Way, galaxies, and so on. Magnetic field in a conducting medium like metal or plasma decays due to Ohmic dissipation. So, how does terrestrial magnetic field, generated by the electric currents flowing in the molten, conducting and rotating core of Earth, prevent itself from Ohmic decay?

Dynamo theories involving differential rotation and convection in conducting fluids are invoked to solve this conundrum. However, Cowling had proved that magnetohydrodynamical flows with axisymmetric geometry will always entail a decaying magnetic field [37]. About two decades later, Backus and Chandra generalized Cowling′s theorem [38]. In this context, Chandra studied the possibility of lengthening the decay duration so that an axisymmetric dynamo provides a feasible explanation for geomagnetism [39]. It was immediately followed by a paper in which Backus showed that the increase was not large enough to be of geophysical interest [40]. Chandra studied several fluid dynamical stability problems employing variational methods that have interesting consequences [41,42].

An evolved binary system, consisting of a Roche lobe[20] filling star, spewing out gaseous matter, and a massive compact object (MCO) like a neutron star or a black hole (BH), both going around the common centre of mass, very often acts as a luminous source of high energy photons. In such a binary system, gas leaking out from the bloated star cannot radially fall on the MCO as it has angular momentum. Instead, it spirals inwards, forming an accretion disc around the MCO so that each tiny gaseous volume element of the disc moves along a circular Keplerian orbit [43].

For a thin disc with a total mass much less than the mass M of the MCO, the Keplerian speed $v(r)$ of a fluid element at a distance r is given by,

$$v(r) = \sqrt{\frac{GM}{r}} \quad , \tag{3}$$

Eq.(3) implies that the fluid elements of the accretion disc rotate differentially. Farther the element from the MCO, lower is its circular speed. Differential rotation leads to viscous rubbing of neighbouring fluid elements at varying distances, causing the accretion disc to heat up. If the disc is sufficiently hot, it emits copious amount of electromagnetic radiation with a spectrum ranging from visible wavelengths to UV photons and X-rays.

There are strong observational evidences that the rapidly time varying, intense X-ray sources, like Cygnus X-1, are accreting black holes (see section VII). Essentially, the gravitational potential energy of the gas spiralling in, gets converted into radiative energy at the rate corresponding to a luminosity of,

$$L = \epsilon \frac{GM\dot{m}}{r_{min}} \quad , \tag{4}$$

where $\dot{m}$, r_{min} and ϵ are the rate of mass accretion, minimum distance reached by the infalling gas and an efficiency factor for the conversion of gravitational energy to radiation, respectively. The importance of accretion on to compact objects is evident from eq.(4), since source luminosity is larger for smaller values of r_{min}. Similarly, a luminous source requires larger rates of accretion and higher conversion efficiency.

For the efficiency factor ϵ to be large, the accretion disc is required to have a high viscosity. The physics of the mechanism responsible for large viscosities in the disc is an active area of research. Interestingly, as shown by Balbus and Hawley in 1991, the Chandrasekhar instability might be the key to the origin of accretion disc viscosity [44]. Chandra had pointed out that a differentially rotating, conducting and magnetized incompressible fluid in a cylindrical configuration, is unstable with respect to oscillating axisymmetric perturbations [41].

While investigating Rayleigh-Benard convection in conducting and viscous fluids threaded with magnetic field, Chandra studied the onset of convection and its dependence on a dimensionless number Q, representing the square of the ratio of magnetic force to viscous force [41]. Today, this number Q is referred to as Chandrasekhar number (or, also as the square of Hartmann number). Chandra made several other contributions in the field of plasma physics and magnetohydrodynamics that had far reaching consequences [45].

VI CHANDRASEKHAR-FRIEDMAN-SCHUTZ INSTABILITY

While studying self-gravitating and rotating fluid configurations, Chandra showed that a uniformly dense and uniformly rotating incompressible spheroid is unstable because of non-radial perturbations, causing emission of gravitational radiation [46]. According to Einstein's general relativity, the curvature of space-time geometry manifests as gravitational force. Gravitational radiations are wave-like perturbations in the space-time geometry that propagate with speed of light, general relativity being a relativistic theory of gravitation. Gravitional waves are radiated whenever the quadrupole moment of the mass distribution in a source changes with time. Friedman and Schutz extended Chandra's findings in 1978, and demonstrated the existence of gravitational wave driven instability in the general case of rotating and self-gravitating stars made of perfect fluid [47].

A physically intuitive way to understand this Chandrasekhar-Friedman-Schutz (CFS) instability is to look at a perturbation mode in a rotating star that is retrograde, i.e. moving in the backward sense relative to the fluid element going around. According to general relativity, the space-time geometry around a rotating body is such that inertial frames are dragged along the direction of rotation (This has been recently verified by the Gravity Probe B satellite-borne experiment [48]). The frame dragging, therefore, would make the retrograde mode appear prograde to an inertial observer far away from the star. Gravitational waves emitted by this mode will carry positive angular momentum (i.e. having the same sense as the angular momentum of the fluid element) as measured in the distant inertial frame. Since, the total angular momentum is conserved, gravitational radiation carrying away positive angular momentum from the mode, would make the retrograde mode go around more rapidly in the opposite direction, leading to an instability.

Andersson in 1998 showed that a class of toroidal perturbations (the so called r-modes) in a rotating star are generically unstable because of the gravitational wave driven CFS instability [49]. Close on heels, it was demonstrated that the r-mode instability would put brakes on the rotation of a newly born and rapidly spinning neutron star [50,51]. Consequently, as the neutron star spins down, a substantial amount of its rotational energy is radiated away as gravitational waves, making it a likely candidate for future detection by the laser interferometric gravita-

tional wave detectors, namely, the LIGOs [52,53]. The CFS instability may soon be put to experimental tests.

VII BLACK HOLES AND GRAVITATIONAL WAVES

In his book on black holes (BHs), Chandra called the astrophysical BHs the most perfect macroscopic objects [54]. Things macroscopic - like chairs, books, computers, etc. around us, require an astronomically large number of characteristics each for their description. For instance, just to specify a suger cube would need not only its mass, density, temperature, but also amount and nature of trace compounds present, the manner in which sugar molecules are stacked, porosity, surface granularities, etc . On the other hand, a BH is characterized by just three physical quantities - its mass, charge and angular momentum.

Schwarzschild BHs do not possess charge or angular momentum, while Kerr BHs rotate but have no charge. On the other hand, Reissner-Nordstrom BHs have charge but do not rotate. Kerr-Newman BHs are theoretically the most general ones, as they possess non-zero mass, charge and angular momentum. Astrophysical black holes are all likely to be Kerr BHs since charge of a BH would get neutralized by the capture of oppositely charged particles present in the cosmic rays and other ambient matter, and since most cosmic objects possess angular momentum. Chandra was particularly fascinated by the stationary, axisymmetric vacuum solutions of Einstein equations that described the Kerr BHs.

BHs are characterized by a fictitious spherical surface called the event horizon centred around the point singularity created by the collapse of matter. Nothing can escape from regions enclosed within the event horizon. For a Schwarzschild BH of mass M, the radius of the event horizon is given by the Schwarzschild radius,

$$R_s = \frac{2GM}{c^2} = 3 \times 10^6 \left(\frac{M}{10^6 \ M_\odot} \right) \text{ km} \quad . \qquad (5)$$

But do BHs exist? Classical BHs by themselves do not radiate. Hawking radiation, which is of quantum mechanical origin, from astrophysical BHs, is too miniscule in amount to be of any observational significance [55]. So, how does one find BHs in nature? In conventional astronomy, their detection relies on the presence of gas or stars in their vicinity and the ensuing stellar or dissipative gas dynamics around an accreting MCO. As discussed in section V, if the MCO has an accretion disc around it like in galactic X-ray sources, quasars, blazars or radio-galaxies, the swirling and inward spiralling gas gets heated up, emitting radio, optical, UV and X-ray photons, often accompanied by large scale jets [56].

If gas can spiral down to a distance $r_{min} = \alpha \ R_s$ from the central BH, then according to eqs. (4) and (5) the radiation luminosity is given by,

$$L = \frac{0.5\epsilon}{\alpha} \dot{m} c^2 \quad . \qquad (6)$$

The real parameter α quantifies the proximity to the central BH. Eq.(6) tells us that accretion taking place close to the event-horizon can convert an appreciable fraction of rest energy mc^2 of the inflowing gas. Higher the accretion rate $\dot{m}$, larger is the luminosity L. (Provided that fluid viscosities in the disc are large enough, as discussed in section V.)

The central engine for a quasar or a blazar is, in all likelihood, an accreting supermassive BH with M lying in the range 10^7- 10^9 $M_\odot$ [56]. Invoking eq.(6) with sufficiently large accretion rates for blazars, one can theoretically explain high luminosities (at times, exceeding 10^{48} erg/s) observed in these sources.

Quasars and blazars also exhibit fluctuating X-ray luminosities on time scales of only few hours. One can derive an upper limit for the size of the central engine from causality arguments. If the observed time scale over which the luminosity varies accreciably is Δt, the size of the source participating in emission of photons cannot be larger than $c\Delta t$. This is because, firstly, every part of the entire region must be causally connected to each other and, secondly, special relativity tells us that parts of the region can physically communicate with each other (to remain in causal touch) only with speeds $\leq c$. X-ray variability on time scales of an hour corresponds to a causal size $\leq 10^9$ km. Now, from eq.(5), a BH of mass 3×10^8 $M_\odot$ has a Schwarzschild radius of about 10^9 km. Short time fluctuations and central engines involving gas dynamics close to the event horizon of BHs, fit together neatly.

Observational evidence for accreting super-massive BHs comes not only from short time variability of X-ray fluxes but also from the details of the continuum spectra (e.g. presence of the big blue bump in quasar spectra) observed in these active sources. Hence, quasars, blazars and powerful radio-galaxies are most probably distant galaxies housing acccreting supermassive BHs with mass in excess of 10^6 $M_\odot$ in their central regions [56].

Similarly, by monitoring stellar dynamics around the central region of Milky Way for decades, one infers that the Galactic nucleus contains a heavy and compact object, most likely to be a supermassive BH with a mass of about 4×10^6 $M_\odot$, within a radius of 10^{13} km from the Galactic Centre [57]. It is interesting to note that the Chandra X-ray observatory (launched on July 23, 1999, and named after S. Chandrasekhar) revealed the presence of a X-ray source as well as hot gas with high pressure and strong magnetic field in the vicinity of the Galactic Centre.

However, these are indirect detections, implying strictly speaking the presence of a very compact, massive central object. Inference of an astrophysical BH,

although very likely, relies on theoretical interpretation. What happens when a BH is perturbed by incident gravitational waves or electromagnetic radiation or Dirac waves describing electrons or neutrinos? Does a perturbed BH have a signature emission like a 'ringing', analogous to the case of a struck bell? To answer such questions, Chandra devoted himself to studying BH perturbations from 1970s onwards [54,60−67].

When a BH is perturbed, the curved space-time geometry around the BH will be subjected to metric fluctuations. For sufficiently small perturbations, a linear analysis of the metric fluctuations can be carried out in terms of normal modes except that dissipation due to both emission of gravitational waves as well as their absorption by the BH make the mode frequencies complex, with the decay reflected in the imaginary parts. In the case of a perturbed BH, such quasi-normal modes (QNMs) correspond to a characteristic ringing that eventually decays due to dissipation.

QNMs were discovered by Vishveshwara [58] and Press [59] while studying gravitational wave perturbations of BHs. Chandra and Detweiler suggested for the first time numerical methods for calculating the QNM frequencies [62] . Such investigations throw light on methods for direct detection of BHs. For example, matter falling into a Schwarzschild BH would lead to excitation of QNMs, resulting in emission of gravitational waves with a characteristic frequency that is inversely proportional to the BH mass.

One can understand this dependence from simple dimensional analysis. QNMs would involve perturbations of the event horizon characterized by the Schwarzscild radius R_s (eq.(5)). So, the oscillation wavelengths would be typically of a size proportional to R_s, making the frequencies depend inversely on the BH mass. A supermassive BH with mass 10^6 $M_\odot$ would ring with a frequency of about 10^{-2} Hz. Because of seismic noise, LIGOs cannot detect gravitational waves having such low frequencies. Only a space-based gravitational wave detector like LISA (Laser Interferometer Space Antenna) can pick up such low frequency signals from supermassive BHs [53,70].

Chandra developed innovative techniques to study BH perturbations, and showed that radial and angular variables could be decoupled to obtain separable solutions for Dirac equation in Kerr background, corresponding to a massive particle (like an electron) [62]. Using similar techniques, Don Page extended the separation of variables for massive Dirac equation to the Kerr-Newman case [68]. In 1973, Teukolsky had separated the Dirac equation for two component massless neutrinos in the Kerr background [69]. It will be interesting to investigate if Chandra's technique can succeed in separating the Dirac equation for massive neutrinos (with flavour mixing and massive right-handed components included) in the Kerr or Kerr-Newman background.

Kerr BHs possess ergosphere, a region surrounding the event-horizon where test particles with negative angular momenta (i.e. with reverse sense of rotation relative to BH rotation) can have negative energy (as measured by a distant inertial observer) orbits. Penrose, in 1969, had shown an ingenious way to extract rotation energy of a Kerr BH that involved sending an object that breaks up into two in the ergosphere, with one of the parts going into a negative energy trajectory, while the other escaping with an energy greater than the initial energy (since energy is conserved) [71].

The wave analogue of Penrose process is superradiance wherein impinging scalar, electromagnetic or gravitational waves emerge out with greater energy after scattering off Kerr BHs. Zel'dovich was the first to show the existence of superradiance in 1970 [72]. Chandra and Detweiler undertook a thorough investigation of scattering of electromagnetic, gravitational and neutrino waves in the Kerr background, and showed that neutrinos do not exhibit superradiance [73]. Absence of neutrino superradiance is most likely due to PEP [73−76].

Exact solutions of two plane gravitational waves colliding with each other were obtained for the first time by Szekeres [77] as well as Khan and Penrose [78]. Their work showed that due to mutual gravitational focusing, the collision leads to curvature singularity where gravity becomes infinite. Chandra, along with Valeria Ferrari and Xanthopoulos, showed that the mathematical theory of colliding gravitational waves can be cast in the form of mathematical theory of BHs, and that the formation of curvature singularity due to gravitational focusing is generic [79−82].

In the later years, Chandra and Valeria Ferrari studied non-radial oscillations of rotating stars taking into account general relativistic effects [83−85]. They showed that the oscillations could be described in terms of pure metric perturbations, reducing the problem to scattering of gravitational waves in curved space-time geometry. For strongly gravitating objects like neutron stars, such gravitational waves may get trapped inside due to deep gravitational potential well, leading to trapped modes that survive for long durations.

In 1983, Chandra was awarded the Nobel prize in Physics. His method of studying diverse astrophysical topics involved applying physical theories that had been corroborated experimentally, and then subjecting the relevant equations to rigorous and innovative mathematical analysis. No wonder that most of the new results he obtained were later confirmed by observations.

References

[1] Fowler, R. H., 1926, Mon. Not. R. Astr. Soc. 87, 114.

[2] Chandrasekhar, S., Astrophys. J. 74, 81 (1931)

[3] Anderson, W., Z. Phys. 56, 851 (1929)

[4] Stoner, E. C. , Phil. Mag. 9, 944 (1930)

[5] S. Chandrasekhar, An introduction to the study of stellar structure, University of Chicago Press, Chicago (1939)

[6] Landau, L., Phys. Z. Sowjetunion 1, 285 (1932)

[7] Also see, Israel, W., in 300 years of Gravitation, eds. S. Hawking and W. Israel (Cambridge University Press, Cambridge, 1987); Srinivasan, G., J. Astrophys. Astr. 17, 53 (1996); Blackman, E. G., arXiv: 1103.1342 [physics. hist-ph]

[8] Baade, W. and Zwicky, F., Phys. Rev. 45, 138 (1934)

[9] Baade, W. and Zwicky, F., Proc. Nat. Acad. Sci. 20, 254 (1934)

[10] Bethe, H. A., Rev. Mod. Phys. 62, 801 (1990)

[11] Demorest, P. B., Pennucci, T., Ransom, S. M., Roberts, M. S. E. and Hessels, J. W. T., Nature 467, 1081 (2010)

[12] Bhattacharya, D., Pramana 77, 29 (2011), and the references therein.

[13] Zhang, W., Woosley, S. E. and MacFadyen, A. I., Astrophys. J. 586, 356 (2003), and the references therein.

[14] Eddington, A. S., Observatory 58, 37 (1935)

[15] A Raychaudhuri, Relativistic cosmology, I, Phys. Rev. 98, 1123 (1955)

[16] Penrose, R., Phys. Rev. Lett. 14, 57 (1965)

[17] Hawking, S. W. and Penrose, R., Proc. Roy. Soc. London A 314, 529 (1970)

[18] Chandrasekhar, S., Astrophys. J. 97, 255 (1943).

[19] Chandrasekhar, S., Astrophys. J. 97, 263 (1943).

[20] Shu, F., Physical Universe (University Science Books, Mill Valley, California, 1982), for a simple explanation.

[21] Binney, J. and Tremaine, S., Galactic Dynamics (Princeton University Press, Princeton, New Jersey, 1987)

[22] David Merritt, arXiv: 1103.5446 [astro-ph.GA], for a recent discussion on generalizing dynamical friction and stellar dynamics to relativistic regime.

[23] Bethe, H., . Phys. 57, 815 (1929)

[24] Wildt, R., Astrophys. J. 89, 295 (1939)

[25] Wildt, R., Astrophys. J. 90, 611 (1939)

[26] Wildt, R., Astrophys. J. 93, 47 (1941)

[27] Chandrasekhar, S., and Krogdahl, M. K., Astrophys. J. 98, 205 (1943)

[28] Chandrasekhar, S., Astrophys. J. 100, 176 (1944)

[29] Chandrasekhar, S., Astrophys. J. 102, 223 (1945)

[30] Chandrasekhar, S., and Breen, F. H., Astrophys. J. 104, 430 (1946)

[31] Chandrasekhar, S., Herzberg, G., Phys. Rev. 98, 1050 (1955)

[32] Chandrasekhar, S., Astrophys. J. 128, 114 (1958)

[33] Chandrasekhar, S., Radiative Transfer (Dover, New York, 1960)

[34] Rau, A. R. P., J. Astrophys. Astr. 17, 113 (1996), and the references therein.

[35] Moehs, D. P., Peters, J. and Sherman, J., IEEE Trans. Plasma. Sci. 33, 1786 (2005), and the references therein.

[36] Holmes, A. J. T., Plasma Physics and Controlled Fusion 34, 653 (1992), and the references therein.

[37] Cowling, T. G., Mon. Not. R. astron. Soc. 94, 39 (1934)

[38] Backus, G. and Chandrasekhar, S., Proc. natn. Acad. Sci. 42, 105 (1956)

[39] Chandrasekhar, S., Astrophys. J. 124, 232 (1956)

[40] Backus, G., Astrophys. J. 125, 500 (1957)

[41] Chandrasekhar, S., Hydrodynamic and Hydromagnetic Stability (Oxford University Press, Oxford, 1961)

[42] Frank, H. Shu, The Physics of Astrophysics, Vol. II (University Science Books, Mill Valley, California, 1992)

[43] Lynden-Bell, D. and Pringle, J. E., Mon. Not. R. Astr. Soc. 168, 603 (1974)

[44] Balbus, S. and Hawley, J., Astrophys. J. 376, 214 (1991)

[45] Parker, E.N., J. Astrophys. Astr. 17, 147 (1996)

[46] Chandrasekhar, S., Phys. Rev. Lett. 24, 611 (1970)

[47] Friedman, J. L. and Schutz, B. F., Astrophys. J. 222, 281 (1978)

[48] Everitt, C. W. F. et al., Phys. Rev. Lett. 106, 221101 (2011)

[49] Andersson N., Astrophys. J. 502, 708 (1998)

[50] Lindblom L., Owen B.J., Morsink S., 1998, Phys. Rev. Letters 80, 4843

[51] Andersson N., Kokkotas K.D., Schutz B.F., Astrophys. J. 510, 2 (1999)

[52] Owen B., Lindblom L., Cutler C., Schutz B.F., Vecchio A., Andersson N., Phys. Rev. D 58, 084020-1 (1998)

[53] Pitkin, M., Reid, S., Rowan, S. and Hough, J., Liv. Rev. Rel. 3, 3 (2000) (arXiv:1102.3355 [astro-ph.IM])

[54] Chandrasekhar, S., The Mathematical Theory of Black holes (Clarendon Press, Oxford, 1983)

[55] Hawking, S., Nature 248, 30 (1974)

[56] Begelman, M. C., Blandford, R. D. and Rees, M. J., Rev. Mod. Phys. 56, 255 (1984)

[57] Schodel, R., Ott, T., Genzel, R., et al. 2002, Nature 419, 694

[58] Vishveshwara, C.V., Nature 227, 936 (1970)

[59] Press, W., Astrophys. J. 170, L105 (1971)

[60] Chandrasekhar, S. and Friedman, J. L., Astrophys. J. 177, 745 (1972)

[61] Chandrasekhar, S., Proc. R. Soc. London A 343, 289 (1975)

[62] Chandrasekhar, S., and Detweiler, S., Proc. R. Soc. London A 344, 441 (1975)

[63] Chandrasekhar, S., Proc. R. Soc. London A 349, 571 (1976)

[64] Chandrasekhar, S. and Xanthopoulos, B. C., Proc. R. Soc. London A, 367, 1 (1979)

[65] Chandrasekhar, S., Proc. R. Soc. London A 369, 425 (1980)

[66] Chandrasekhar, S. and Xanthopoulos, B. C., Proc. R. Soc. London A, 378, 73 (1981)

[67] Chandrasekhar, S., Proc. R. Soc. London A 392, 1 (1984)

[68] Page, D. N., Phys. Rev. D 14, 1509 (1976)

[69] Teukolsky, S. A., Astrophys. J. 185, 635 (1973).

[70] Ferrari, V. and Gualtieri, L., Gen. Rel. Grav. 40, 945 (2008)

[71] Penrose, R., Rev. Nuovo Cimento 1 (Special number), 252 (1969)

[72] Zel′dovich, Ya. B., JETP Lett. 14, 180 (1971)

[73] Chandrasekhar, S., and Detweiler, S., Proc. R. Soc. London A 352, 325 (1977)

[74] Unruh, W., Phys.Rev.Lett. 31, 1265 (1973)

[75] Iyer, B. R. and Kumar, A., Phys. Rev. D 18, 4799 (1978)

[76] Chandrasekhar, S., in General Relativity: An Einstein Centenary Survey, eds. S. W. Hawking and W. Israel (Cambridge Univ. Press, New York, 1979)

[77] Szekeres, P., Nature 228, 1183 (1970)

[78] Khan, K. A. and Penrose, R., Nature 229, 185 (1971)

[79] Chandrasekhar, S. and Ferrari, V., Proc. R. Soc. London A 396, 55 (1984)

[80] Chandrasekhar, S. and Xanthopoulos, B. C., Proc. R. Soc. London A 408, 175 (1986)

[81] Chandrasekhar, S. and Xanthopoulos, B. C., Proc. R. Soc. London A 410, 311 (1987)

[82] Chandrasekhar, S., Selected Papers, Vol. 6 (The University of University Press, Chicago, 1991)

[83] Chandrasekhar, S., and Ferrari, V., Proc. R. Soc. London A 432, 247 (1991)

[84] Chandrasekhar, S., and Ferrari, V., Proc. R. Soc. London A 434, 449 (1991)

[85] Chandrasekhar, S., and Ferrari, V., Proc. R. Soc. London A 433, 423 (1991)

* patrick@srb.org.in

The challenging concept of time in quantum mechanics

Jafari Matehkolaee, Mehdi
Islamic Azad university of Shahrood, Sharood, Iran
mehdisaraviaria@yahoo.com

(*Submitted* Feb 2011)

Abstract

Time plays a peculiar role in quantum mechanics. What makes this concept so interesting is the question "what can quantum mechanics tell us the about the nature and role of time?" and conversely, "what can time tell us about the structure of quantum theory?" In standard quantum mechanics probabilities are assigned to measure the outcomes of a given observable at a given moment of time. Time enters the Schrodinger equation as an external parameter, and not a dynamical variable. It is not a standard quantum mechanical observable. But in concepts such as the time of arrival , the time-energy uncertainty relation , tunneling time , and time in quantum gravity , time can no longer be viewed as a mere parameter. This survey explores various attempts made in order to treat time as a dynamical variable (observable) and hence measure it.

.

I. Introduction

What is time? This is a very old philosophical question. Even Einstein had a hard time answering this question, but in spite of that, we can measure time more accurately than any other quantity. Atomic clocks are the most accurate timepieces ever made, and are essential for such features of modern life as synchronization of high speed communication and the operation of the Global Positioning System (GPS) that guides aircraft, cars and so on."

The role of time is a source of confusion and controversy in quantum mechanics [1]. In the Schrodinger equation time represents a classical external parameter, not a dynamical variable. The time measured in experiments, however, does not correspond to an external parameter; it is actually an intrinsic property of the system under consideration, which represents the duration of a physical process; the life time of unstable particles is a well-known example. Quantum mechanics was initially formulated as a theory of quantum micro-systems interacting with classical macro systems [2]. Quantum mechanics allows the calculation of dynamical variables of systems at specified instants in time using the Schrodinger equation [3]. The theory also deals with probability distributions of measurable quantities at definite instants in time [4]. The time of an event does not correspond to a standard observable in quantum mechanics [5].

Asking the question of when a given situation occurs, time is no longer an external parameter. Time, in such a situation, becomes dynamical. However, such a time observable does not have the properties of a "standard" quantum mechanical observable. This research is dedicated to exploring various attempts made in order to treat time as a dynamical variable (observable). All attempts use essentially one of two approaches, namely those of direct and indirect the measurement of time. Direct approaches use theoretical toy model experiments while indirect approaches are of mathematical nature. The controversy of time arises in the time of arrival concept, the search for

a time operator, the time-energy uncertainty relation and the tunneling time. A very important issue as well is the role of time in the context of quantum gravity. The problem of time in quantum gravity also opens the door to the ever-lasting question: what is time?

To determine the time of arrival or the tunneling time, the measurement of the required quantities must always be done, directly or indirectly. The notion of measurement emerges from interpretations of quantum mechanics, however the time problem arises in all of them. The interaction of a quantum Microsystems with a classical macro system is described in terms of quantum measurements [2]. As time is treated as an external parameter in standard quantum theory, quantum observation theory talks about observations made at given instants in time [3]. The system in standard quantum theory interacts with a measuring device through the time dependent interaction Hamiltonian. Quantum mechanics is actually designed to answer the question "where is a particle at time t?" In standard quantum mechanics, the probability corresponds to a measurement result of a particle being at a given location at one specific time. The above mentioned micro-system is taken to be in a superposition of states of its variables. Suppose the macro-system interacts with one of the micro-system's variables, then the macro-system only sees one of the many possible values of the variable [2]. The interaction itself projects the state of the micro-system into a state with the given value. In terms of wave-functions, the interaction (act of measurement) causes the wave-function of the Microsystems (a superposition of states) to "collapse" into one state with a specific value (eigenvalue). Dirac mentioned that the superposition is one of two most important concepts in quantum mechanics; the other one is Schrodinger equation [6]. Even though several alternative interpretations have been devised (Bohm, many- worlds, etc.), they all have one problem in common: how can the exact time at which a measurement occurs be determined? Rovelli [2] illustrates how the problem of time arises in each interpretation. If a system is viewed as having a wave-function which collapses during a measurement, is the collapse immediate? If a system is viewed in terms of values of its dynamical variables which become definite when observed, how to determine exactly when this occurs in an experiment? If a system's wave-function is taken a branch, when does this occur? If a wave-function does not branch and the observer selects one of its components and sticks with the choice, when does the selection occur? If there exists probability for sequences of events to happen, when does such an event occur? The above questions indicates the universality and challenging concept of time. In section II, The concept of time of arrival, in the context of quantum mechanics is discussed. The issue of time arises also in Heisenberg's time-energy uncertainty relation (section III). This relation has direct consequences to defining a time operator. Another important concept is tunneling time (section IV). It is purely quantum mechanical phenomenon with no classical analogue. Many of the ideas president in the context of the time arrival can be carried over to tunneling time. In section V, we review some attempts to set up the time operators. Last but not least the, problem of time in quantum gravity is outlined, where time, if it is a fundamental variable, must also be a dynamical variable. Quantum gravity has the interesting feature that the philosophical question of what time actually is raised (section VI). If one would know what time is fundamentally, then perhaps the problems encounter in determining time in quantum mechanics could be solved, as one would then know what one is actually looking for. In what follow, we only highlight the subjects, and to understand more each part needs to be explored in details. Another approach to the time problem is the decoherent histories approach to quantum mechanics [7, 8, 9, 10]. This formalism makes use of the fact that what one considers to be a closed quantum system, is never completely closed, as there always is an interaction present with the

environment. The Brownian motion model is the main idea presented in this context [7].

II. Time of Arrival (TOA)

II. 1. Time of Arrival in Classical Mechanics

The basic question to answer is, can the exact time be measured at which a particle arrives at a specified point? Taking a beam of free particles, a measurement needs to be done to find the time of arrival at the specified point $x = x_1$. An experiment can be constructed which involves a clock positioned at the point $x = x_1$ This clock will turn itself off when a particle reaches x_1. In classical mechanics the time of arrival can be measured in this way with extreme accuracy, as the non-vanishing interaction between the particle and the clock is very small. The time of arrival can also be measured indirectly in classical mechanics. The equation of motion of the particle is inverted to get time as a function of location x and momentum p:

$$T_1 (x (t) , p (t) , x_1) \qquad (1)$$

This can be evaluated at any time *t* by measuring p(t) and x(t) simultaneously. Classically direct and indirect measurements are completely equivalent. Both methods give exactly the same result [11]. Muga et al [12] give an example of a particle moving in one dimension with position q and momentum p. The particle's trajectory might cross a given point X only once if no reflection mechanism is present. If a potential barrier is introduced, it can reflect the particle's trajectory and cause it to cross the point X more than once. The first passage time is defined as the first crossing of the trajectory of the point X. Considering ensembles of non-interacting particles, Muga et al state that a distribution of times is associated with the nth passage given by the nth crossing. A phase space distribution F(q,p,t) can be used to describe an ensemble of free moving, non-interacting particles. The distribution is normalised to one and is defined such that it only considers particles moving towards the right: $F (q, p \leq 0) = 0$. The particle trajectories cross the point X only once and a current density J(X, t) at X and time t (probability flux) gives the distribution of the first passage arrival times. Let J(X, t) dt be the fraction of particles which cross X between t and t+dt. Defining

$$J(X,t) = \int_{-\infty}^{\infty} F\ (X,p,t)\frac{p}{m}\,dp \qquad (2)$$

and the trajectory equation $q(t) = q_0 + \frac{pt}{m}$, the average time for free motion is given by

$$\int j(X,t)tdt = \iint F(q_0,p,0)\,\frac{(X-q_0)m}{\rho}\,dq_0dp$$

The integral is well-defined if F cancels the singularity.

II.2. Time of Arrival in Quantum Mechanics

The time of arrival problem in quantum mechanics arises by turning around the question: "at what time is the particle at a specified location?" Attempts to answer this question raise several problems which lead to ambiguous answers. The best way to illustrate this is through a simple example [5]:

Consider a N-particle ensemble. The aim is to measure the time at which a particle is located at the point x. A simple way of doing this would be to consider a detection process where the detector is switched on by each particle only at a given time t=T. Then this process is repeated on a second ensemble at $t = T^1$ and so on. The probability of finding the particle

$$\left|\psi(x,t=T)\right|^2 \text{ and } \left|\psi(x.T\right|^2 N = n_T \qquad (4)$$

is the average number of particles found at position x at time t =T. Unfortunately, (4) does not represent a probability as it is not normalised properly. To overcome this problem consider

$$\frac{\left|\psi(x.t\right|^2}{\int\left|\psi(x.t^1\right|^2 dt^1} \qquad (5)$$

However, to be able to use this equation, the state

ψ(x,t) must be known at all times in the past and in the future. The reason for the problem is that the particle could be at the point x at several times. For example, if the particle is found at point x at time t_1 with probability one, it is not possible to say that the particle was not at x at all other times.
To try to overcome the above mentioned difficulty the measurement of the time of arrival of a particle at a given point seems a good candidate, as a particle can arrive only once at a given location. To measure the time of arrival of a particle, it must be possible to be able to detect it at a given point, as well as knowing that is was not there before the measurement takes place. This requires a continuous monitoring of the point of arrival. Now the problem arises that the probability of detecting a particle at a time $t = t_1$ is not independent of detecting it at $t = t_2$. In mathematical terms the projections onto the arrival position x, denoted by the projection operator P_x, at given times t_1 and t_2 will not commute:

$$[P_x(t_1), P_x(t_2)] \neq 0$$

This means that the measurements that are done at different times do not commute and disturb one another. This also means that (5) is not a probability distribution in time.

III. Uncertainty Principles

III.1. Introduction

In trying to change time, as the classical external parameter, into an observable, one cannot deduce the time-energy uncertainty relation:

$$\Delta t \Delta E \geq \frac{\hbar}{2}; \qquad (7)$$

where t = time , E = energy from kinematical point of view, as time does not belong to the algebra of observables [12]. In spite of this, (7) is generally regarded as being true. The relation (7), unlike other canonical pairs, is not the consequence of fundamental quantum in-complementarity of two canonical variables. The time-energy uncertainty relation is very different to the standard quantum uncertainty relation, such as the position momentum one. The precise meaning of the time-energy relation is still not exactly known. The problem lies in the fact that one cannot give the precise meaning to the quantity Δt . This is because time is not a standard quantum mechanical observable associated with an Hermitian operator. If such an operator canonically conjugate to the Hamiltonian did exist, then, t could be defined conventionally and the uncertainty principle could be applied to the physical quantity corresponding to the time operator.

III.2. Quantum Mechanical Uncertainty

In classical mechanics any quantity can be measured to an arbitrary precision In quantum mechanics the same is possible by preparing a quantum system in a well defined state of position and hence perform a measurement which reveals where the particle is located very accurately. The difference from classical mechanics arises when the values of two different observables are desired to be determined. In classical mechanics there is no reason why two quantities cannot be measured with high precision. In quantum mechanics only compatible (commuting) observables can be measured simultaneously. In general the uncertainties in measurements of two observables obey the uncertainty relation, which creates a lower bound on the product of the individual uncertainties, which is not equal to zero. For any two observables $\hat{A}$ and $\hat{B}$, their uncertainties

$$\Delta\hat{X} = \left(\langle\hat{X}^2\rangle - \langle\hat{X}\rangle^2\right)^{1/2}$$

are used to derive the uncertainty relation [13]:

$$\Delta\hat{A}\Delta\hat{B} \geq \frac{|\langle[\hat{A},\hat{B}]\rangle|}{2} \qquad (8)$$

An important fact that should be noted is that the uncertainty. $\Delta\hat{X}$ of an observable $\hat{X}$ is an intrinsic property of any quantum state .

III.3. Heisenberg's Uncertainty Principle

The uncertainty principle expresses the physical content of quantum theory in a qualitative way

[13]. The uncertainty principle was first proposed by Heisenberg in 1927. It basically states that is not possible to specify exactly and simultaneously the values of both members of a pair of physical variables which describe the behavior of an atomic system. In a sense the principle can also be seen as a type of constraint. The members of a pair are canonically conjugate to each other in a Hamiltonian way. The most well known example is the coordinate x of a particle (position in one dimension) and its corresponding momentum component P_x:

$$\Delta x \Delta p_x \geq \frac{\hbar}{2} \qquad (9)$$

Another example is the angular momentum component J_z of a particle and the angular position ϕ in the perpendicular (x,y) plane:

$$\Delta\phi \Delta J_z \geq \hbar \qquad (10)$$

In classical mechanics these extreme situations complement each other and both variables can be determined simultaneously. Both variables are needed to fully describe the system under consideration. In quantum theory, Eqn. (9) states that one cannot precisely determine a component of momentum of a particle without loosing all information of the corresponding position component at a specific time. If the in- between extremes case is considered, the product of the uncertainty in position and the uncertainty in the corresponding momentum must numerically be equal to, at least, $\hbar/2$

To understand the physical meaning of the uncertainty principle, Bohr in 1928 stated the complementary principle. This principle shows the fundamental limits on the classical concept that a system's behaviour can be described independently of the observation procedure. The complementary principle states that "atomic phenomena cannot be described with the completeness demanded by classical dynamics" [13]. Basically the principle states that experimental apparatus cannot be used to determine a measurement more precisely than the limit given by the uncertainty principle. In a sense when a measurement is done to determine the value of one of a pair of canonically conjugate variables, the second variable experiences a shift in value. This shift cannot be calculated exactly without interfering with the measurement of the first variable

III.4. The Relation of the Uncertainty Principle to a Time Operator

Bohr also realized that the two uncertainty principles (9) and (7) can be interpreted in two different ways; the first is as limitations on the accuracy of a measurement and the second is as statistical laws referring to a large sequence of measurements. The difficulty in giving meaning to the relation (7) is due to the quantity Δt. In the way it is interpreted above, the uncertainty relation (7) implies the existence of a self-adjoint operator, canonically conjugate to the Hamiltonian $\hat{H}$, which itself is self-adjoint. If this time operator $\hat{T}$ exists, then the quantity Dt can be interpreted in the same way as Dx or Dp_x and the uncertainty principle can be applied to the physical observable corresponding to T. To obtain the uncertainty relation for energy and time, the commutator of the Hamiltonian and the time operator is assumed to be of the form:

$$[\hat{H},\hat{T}] = i\hbar \qquad (11)$$

The form of (11) is such that $\hat{T}$ and $\hat{H}$ are canonically conjugate to each other. It also implies that both operators have a continuous spectrum. This in turn means that neither of the two can be a Hamiltonian, as such an operator is defined to have a semi- bounded spectrum. From this line of reasoning the supposed time operator $\hat{T}$ cannot exist. This problem is encountered when one uses (11) to derive the uncertainty relation (7) in the same way as (9) is derived from $[\hat{x},\hat{p}] = i\hbar$ [14].

IV. Tunneling Time

In quantum tunneling, a part of a particle's wav-function has a significant probability of being transmitted a potential barrier, even if its energy is

less than the energy of the top of the barrier [15]. This is not true classically, hence tunneling is a purely quantum phenomenon where a particle has the probability of moving through classically forbidden regions. The transmission probability of a particle's wav eigenfunction is calculated from the time-independent Schrodinger equation. The problems arise when time dependence is required. The root of the problem of time dependence lies in the uncertainty relation. However, the fundamental problem is that in quantum mechanics, there exist no real physical paths along which a particle moves. This problem seems a logical basis to employ the method of Feynman path integrals, which are virtual paths in configuration space [16]. The path integral approach to the tunneling time , yielding a complex time, is due to Sokolovski and Baskin [17] .

The question "how long does a particle spend a potential barrier?" has been controversial for many years [18] (for an extensive review see [19]. Part of the controversy lies in the fact that in tunneling processes only a particles tunnel, so one cannot discuss the entire ensemble. Over the years there have been many different approaches to calculate tunneling time; among them are the path integral approach, physical clock gedanken experiments, and consistent (decoherent) histories approach. There have also been attempts to use interactions of wave-packets with the barrier [15]. Yamada [16] studies the tunneling time problem using the decoherent histories approach to quantum mechanics to define the probabilities for histories. To minimize the interference, such that probabilities can be assigned to histories, Yamada uses the weak de coherence condition, where only the real part of the decoherence functional is required to vanish. Along with the decoherence condition, he [20] imposes that the initial condition satisfies the decoherernce condition as well.

Attempts to construct a Time Operator

Standard quantum theory, as proposed by Pauli [21], requires that measurable quantities (observables) are represented by self-adjoint operators, which act on the Hilbert space of physical states [4]. The probability distribution of the measurement outcomes of an observable are obtained as "an orthogonal spectral decomposition of the corresponding self-adjoint operator" [4]. The indirect measurement of time basically is the quest of finding a self-adjoint operator whose eigenstates are orthogonal. As the time operator is one of the canonically conjugate pair of time and energy, the time operator must be defined in such a way as to preserve the semi bounded spectrum of the Hamiltonian. Pauli pointed out [2 L] that the existence of a self-adjoint time operator is incompatible with the semi-bounded character of the Hamiltonian spectrum. By using a different argument based on the time-translation property of the arrival time concept, Allcock has found the same negative conclusion [22-24]. The negative conclusion can also be traced back to the semi-infinite nature of the Hamiltonian spectrum.

Kijowski [25] tried different approaches to find a time operator. He chose to (interpret the uncertainty relation (11) in a statistical way.

Grot, Rovelli and Tate [26] construct a time of arrival operator as the solution to the problem of calculating the probability for the TOA of a particle at a given point. They argue, using the principle of superposition, that a time operator T can be defined, whose probability density can be calculated from the spectral decomposition of the wave-function l. y(x) into eigenstates of $\hat{T}$ (in the usual way). They found an uncertainty relation which approaches (11) to arbitrary accuracy. Oppenheim, Reznik and Unruh [27] follow the method by Grot at al. They used coherent states to create a positive operator valued measure (POVM). The standard method to find an operator is by using the correspondence principle, which states that the corresponding classical equations are quantized using specific quantization rules. Taking the Hamiltonian of a classical system H(p,q) where p and q are canonical variables (H,T), where H is the

Hamiltonian and T is its conjugate variable. These variable satisfy Hamilton's equation:

$$\frac{dT}{dt} = \{H, T\} = 1 \qquad (12)$$

where T is the interval of time and the curly brackets denote a Poisson bracket. This relation can be translated to quantum mechanics through canonical quantization. This is a procedure where classical expressions remain valid in the quantum picture by effectively substituting Poisson brackets by commutators:

$$\{H, T\} = \frac{1}{i\hbar}\,[\hat{H}, \hat{T}\,] \qquad (13)$$

In the Heisenberg picture H and T are hence interpreted as self-adjoint operators. Further it seems natural to require that the time operator satisfies an eigenvalue equation in the usual way:

$$\hat{T}(t)\rfloor t_A\rangle = t_A\rfloor t_A\rangle \qquad (14)$$

In all of physics, except in General Relativity, physical systems are supposed to be situated in a three-dimensional Euclidean space. The points of this space will be given by cartesian coordinated **r** = (x, y, z). Together with the time parameter t, they from the coordinates of a continuous space - time background. The (3 + 1) dimensional space-time must be distinguished from the 2N-dimensional phase space of the system, and space-time coordinates (r, t) must be distinguished from the dynamical variables (q_k, P_k) characterizing material systems in space-time.

A point particle is a material system having a mass, a velocity and acceleration, while r is the coordinate of a fixed point of empty space. It is assumed that three dimensional space is isotropic (rotation symmetric) and homogeneous (translation symmetric) and that there is translation symmetry in time. In special relativity the space-time symmetry is enlarged by Lorentz transformations which mix **x** and t, transforming them as the components of a four-vector.
The generators of translation in space and time are the total momentum P and the total energy H, respectively. The generator of space rotations is the total angular momentum **J**.

It is worth noting that the universal time coordinate t should not be mixed with dynamical position variables. The important question to ask is: Do physical systems exist that have a dynamical variable which resembles the time coordinate t in the same - way as the position variable q of a point particle resembles the space coordinate **x**? The answer is yes! Such systems are clocks. A clock stands, ideally, in the same simple relation to the universal time coordinate t as a point particle stands to the universal space coordinate **x**. We may generally define an ideal clock as a physical system which has a dynamical variable which behaves under time translations in the same way as the time coordinate t. Such a variable, which we shall call a "clockvariable" or, more generally, a "time-variable", may be a pointer position or an angle or even a momentum. Just as a position-variable indicates the position of a system in space, a clock-variable indicates the 'position' of a system in time t. In quantum mechanics the situation is essentially not different. The theory supposes a fixed, unquantized space-time background, the points of which are given by c-number coordinates **x**, t. The space time symmetry transformations are expressed in terms of these coordinates.

Dynamical variables of physical systems, on the other hand, are quantized: they are replaced by self-adjoint operators on Hilbert space. All formulas of the preceding section remain valid if the poisson-brackets are replaced by commulators according to

$$\{,\} \rightarrow (i\hbar)^{-1}\,[\,,\,].$$

So, the idea, that t can be seen as the canonical variable conjugate to the Hamiltonian, leads one to expect t to obey the canonical commutation relation $[t,H] = i\hbar$. But if t is the universal time operator it should have continuous eigenvalues running from $-\infty$ to $+\infty$ and, from this, the same would follow for the eigenvalues of any H. But we know that discrete eigenvalues of H may occur.

From this Pauli concluded [21]: ... that the introduction of an operator t is basically forbidden and the time must necessary be considered as an ordinary number ("c-number"). Thus, the 'unsolvable' problem of time in quantum mechanics has arisen. Note that it is crucial for this argument that t is supposed to be a universal operator, valid for all systems: according to Pauli the introduction of such an operator is basically forbidden because some systems have discrete energy eigenvalues. From our previous discussion it should be clear that the universal time coordinate t is the partner of the space coordinates x. Neither the space coordinates nor is the time coordinate quantized in standard quantum mechanics. So, the above problem simply doesn't exist! If one is to look for a time operator in quantum mechanics one should not try to quantize the universal time coordinate but consider time-like (in the literal sense) dynamical variable of specific physical system, i.e. clocks. Since a clock-variable is an ordinary dynamical variable quantization should not, in principle, be especially problematic. One must, however, be prepared to encounter the well-known quantum effects mentioned above: a dynamical system may have a continuous time-variable, or a discrete one or no time-variable at all. Recently, some efforts have been advanced to overcome Pauli's argument [28]. The proposed time operator is canonically conjugate to $i\hbar\partial$ rather than to H, therefore Pauli's theorem no longer applies. It is argued that "the reasons for choosing time as a parameter lie not so much in ontology as in methodology and epistemology. The time operator idea needs to be more explored in an accurate way.

VI. The problem of Time in Quantum Gravity

VI. l. The basic problem

The problem of time is a fundamental concept that needs to be considered in quest for a consistent theory of quantum gravity [29]. The main issue contributing to the problem of time is the invariance of classical general relativity under space-time diffiomorphism. This means that the invariance contradicts the Newtonian image of a fixed, absolute time parameter. This situation is encountered in all theories, which have a classically invariant, reparametrization of time [30]. This leads to time disappearing when quantizing the theory. This situation comes out to the question of what to make of the classical Hamiltonian constraint in the quantum version of the theory. Basically, if time is a fundamental concept, then it must be a dynamical variable of the theory.

As stated above, when quantizing general relativity in a canonical way, time seems to have no fundamental notion. Isham [29] summarizes the key points in four statements: 1. How should time re-enter quantum gravity theory? 2. Should time be defined classically before quantization? Or 3. Should it be defined after quantization? 4. If time is not the fundamental quantity, which it is said to be, how relevant is quantum mechanics when dealing with time? The definition of time also has a direct effect in quantum cosmology, The main problem is the Newtonian concept of time, which is replaced by the concept of an internal time in many approaches of problem of time in quantum gravity.

The problem of time in quantum gravity arises when one wants to quantize general relativity. The canonical quantization method involves expressing general relativity in Hamiltonian from, to then apply a quantization scheme. General relativity is a theory with constraints, which generate asymmetry. Such theories are invariant under the reparametrization of time. The action of such a system is invariant under canonical transformations.

One can proceed to quantize general relativity in Hamiltonian from using Dirac's proposal and functional Schrodinger quantization to find all the information contained in the constraints. Using the metric representation of the wave-function, one obtains the Wheeler- DeWitt equation. This equation shows the absence of time. One way to

interpret this is to consider that as general relativity is a parametrized theory, physical time is already contained amongst the dynamical variables. All such theories have H = 0. Alternatively, there exists a geometric interpretation.

VII. Conclusion and further comments

This survey explores various ways of defining time in standard quantum mechanics and some different ways of measuring it. The approaches of measuring time yield a whole spectrum of results along with a range with a range of difficulties encountered. All methods yield results which have a strict limit on their accuracy and generality. This reflects the quantum nature of the problem.

The main difficulty in defining a quantum time operator lies in non-existence, in general, of a self-adjoint operator conjugate to the Hamiltonian, a problem which can be traced back to the semi-bounded nature of the energy spectrum. In turn, the lack of a self-adjoint time operator implies the lack of a properly and unambiguously defined probability distribution of arrival time. There are two possibilities to overcome the problem. If one decides that any proper time operator must be strictly conjugate to the Hamiltonian, then one has to perform the search for a self-adjoint operator. If, on the contrary, one imposes self-adjoint property as a desirable requirement for any observable, then one necessarily has to give up the requirement that such an operator be conjugate to the Hamiltonian. The two main equations of motion, the Schrödinger and wheeler- Dewitt equation, reflect two different presupposed natures of time: in the schrödinger equation, time corresponds to an external parameter and in the Wheeler-deWitt equation there is no time. This research explores the concept of trying to tum a time parameter into an observable, a dynamical variable. Why was time in quantum mechanics represented by a parameter in the first place? A possible answer is that it is due to our perception. It is meaningful, for us, to talk about events happening at a certain time. This lets us put events into a chronological order in our minds. We do not think about an event happening to us. Another question is, why does one want time to be an observable? One major reason is our notion of change: we seem to perceive that time changes. Another motivation for the study of time in quantum mechanics is the problem of time in quantum gravity. Quantum cosmology represents an analogy to closed quantum systems, as both cosmology and closed quantum systems are describing the same type of situation, the difference being the size scale. . Saunders states: "quantum cosmology is the most clear-cut and important failing of the Copenhagen interpretation" [31]. Perhaps the lack of understanding of time in quantum gravity is due to a fundamental reason, based on the two quantum gravity components: quantum mechanics and general relativity. The problem does not lie in general relativity however, so it must be rooted in the formulation of quantum mechanics.

Quantum theory of measurement is based on measurements occurring at given instants of time. A measurement corresponds to a classical event. Dirac said "the aim of quantum mechanic was to account for the observables: behavior in the simplest possible ways" [6]. Kant [32] held Newtonian absolute space and space- time for an "idea of reason". Saunders states" In particular, we need a global time coordinate' which enters in to the fundamental equations; it is no good if this involves ad hoc or ill-defined approximations, available at only certain length scales or cosmological epochs" [33]. His idea of a universal definition of time sounds very appealing. Does this universal concept of time require the reformulation of quantum mechanics? Tunneling time might .also be a candidate to shed some light on to the mystery of time. Quantum mechanical tunneling is "one of the most mysterious phenomena of quantum mechanics" and at the same time it is one of the basic and important processes in Nature, party responsible for our existence [34]. The question of the duration of a tunneling process is an open problem. Experiments to record the tunneling time were

motivated by the many different theories trying to describe this phenomenon. Questions arise such as, "is tunneling instantaneous?","is it subluminal or superluminal (faster than the speed of light)?" Chiao published a paper with experimental evidence that tunneling is superluminal [34]. If this is true, what implications does superluminal tunneling have on our understanding of the nature of . time? What does it mean to say that something happens faster than instantaneously?

Does time undergo a change in nature when it "enters" a classical forbidden region? If so, what is it and what does it change to?

In quantum gravity, the evolution of the gravitational field does not correspond to evolution in physical time. The internal time on a manifold i~ not ':l:~ absolute quantity. Barbour [35] claims that an instant in time corresponds to a configuration and Deutsch, in his interpretation of quantum mechanics, claims that a change in time corresponds to a change in his interpretation of quantum mechanics, claims that a change in time corresponds to a change in the number of Deutsch worlds [37]. Is it possible that the notion of absolute time be a hint towards timelessness? If time does not exist then the various different formulations of the nature of time only appear through our perception and we cannot follow these back to a universal truth. Perhaps there does exist a universal concept of time, which is far too abstract to grasp. Whatever time may be, the time discussed in this overview raise various questions, which perhaps are trying to point us into .a certain direction. Trying to answer questions about the concepts of the time of arrival, the time-energy uncertainty relation, tunneling time and time in quantum gravity show us that perhaps nothing is more important than to first of all understand the basic building block-time-without which no structure can be perfectly built. The problem of time still stands to be resolved, the quest for this research still continues.

References

1. Muga, J.G., S.Brouard and D. Macias, Ann. Phys. 240, 351-361 (1995).
2. Rovelh.C., Found. Phys. 28,1031 (1998
3. Bloch, 1. And D. A. Bueba, Phys. Rev. DIO, 3206(1973).
4. Delagado, V., and J.G . Muga, Phys. Rev. A56, 3425(1997)
5. Oppenheim, J., B. Reznik and W.G. Unruh, quanti 9807058V2, Time as an observables
6. Dirac, P., "The principles of Quantum Mechanics", Oxford university press (1930).
7. M. R. sakardei: Can. J. Phys. 82, 1-17 (2004)
8. Halliwwll, J.J. Aspects of the Decoherent Histories Approach to quantum Mechanics, in Stochastic Evolution of Quantum States in Open systems and Measurement Processes, edited by L.Diosi, L.and B. Lukacs (World Scientific, Singapore, 1994).
9. Halliwell, J.J. and E.Zafiris, Phys. Rev. D57, 3351(1998).
10. Yamada, N., in the continuous consistent history approach to the tunneling time problem, World Scientific, Singapore, (1997).
11. Aharonov, J., J. Oppenheim, S. Popescu, B. Reznik, and W.G. Unruh, quantph/9709031; Measurement of Time of Arriaval in Quantum Mechanics.
12. Muga, J.G., R.Sala and J. Palao, Superlattices Microstruct., 833 (l998)
13.Schiff, L.1., "Quantum Mechanics", McGraw-Hill, (1968)
14.Greiner,W.,"QuantumMechanicsaninteroductio n", 3rd edition, (1994)
15. Marinov, M.S., and B. Segev, quant-ph/9603018, on the concept of tunneling
16.Yamada, N., in the continuous consistent history approach to the tunneling
time problem, World Scientific, Singapore, (1997).
17.Sokolovski, D. and L. M. baskin, Phys. Rev. A36, 4604 (1987).
18. Steinberg, A.M., quant-phl9502003, conditional probabilities in quantum
theory, and the tunneling time controversy

19. Hauge, E.H. and lA. Stovenge, Rev. Mod. Phys. 61, 917(1989).
20. Yamada, N. Phys. Rev. A54, 182(1996).
21.Pauli, W. Encyclopaedia of Physi cs, Berlin; S ingapore, P. 60(19 58).
22. Allcock, G.R. Ann. Phys. 53,253(1969) .
23. Allcock, G.R. Ann. Phys. 53, 286(1969).
24. Allcock, G.R. Ann. Phys. 53, 311 (1969).
25. Kijowski, l Rep. Math.Phys. 6, 361(1974).
26.Grot, N., C. Rovelli and R.S. Tate, Phys. Rev. A54, 4679(1996).
27.Oppenheim, J., B. Reznik and W.G. Unruh, quant-phl9807043, Time-ofArrival States.
28. Wang, Z.Y., B. Chen, and C.D. Xiong, [Time in quantum mechanics and quantum field theory], J. Phys. A:Math. Gen. 36,5135-5147(2003).
29. Isham, C.l gr-qc/9210011, Canonical quantum gravity and the problem of time.
30. Barbour, J. The end of time: The next revolution in our understanding of the Universe, (Weidenfeld and Nicholson, 1999).
31. Saunders, S. Time and quantum mechanics, in Now, time and quantum mechanics, edited by M. Bitbol and E. Ruhnau, Editions Frontiers, P.21. (1994).
32. ref. [31], P.27.
33. ref. [31], P.45.
34. Chiao, R.Y. quant-ph/98110 19, tunneling times and superluminality: a Tutorial.
35.ref. [30],P.1.
36. Deutsch, D. Int. Jouro. of Theor. Phys. 24,1(1985).

Teaching of Faraday's and Lenz theory of electromagnetic induction using java based Faraday's laws of stimulations.

Sanjay Prakashchand Hargunani
Department of physics, G.S.Arts, Commerce and science College,
Khamgaon- 443201 Maharashtra state India
E-mail: sanjayhargunani@rediffmail.com

(*Submitted* July 2010)

Abstract

I have used Faraday's lab simulation software freely available on website http://phet.colorado.edu to teach faraday's and Lenz's theory of electromagnetic induction. I had taken the sample of 30 students and 30 questions. Student's response to all questions before and after simulation was noted to study effect of simulation lab work. The response of students to conceptual and application oriented questions was totally changed. They realize their mistakes in understanding of EMI phenomenon. Teaching with faraday's lab simulation creates the interest and curiosity about EMI among students. It makes the study Easy and reduces the real lab work. It is difficult for high school teachers to realize every concept of EMI in real lab experiments due to limited resources. This simulation helps the students to learn the EMI phenomenon by their own.

Keywords: Physics education, electromagnetic induction, faraday's lab simulation

I. INTRODUCTION

School teachers teach the Faraday's and Lenz's theory of electromagnetic induction using equations, graphs, diagrams, examples and numerical. Many students face considerable difficulties in understandings the phenomenon using equations. Student use equations to calculate some variables and numbers as a solution. It is very difficult for students to see the importance of each variable and constants in a given equations. However physical equations have deeper meanings. Equations represent the relation between various observations and measurements. By using simulation based experiments; student can see the important of each variable of equation. Such simulation based teaching changes the students view about equations. Students can imagine lot of things just from equations. Simulation base teaching enhances the visualizations power of students for physical phenomenon. Student can solve the practical problems after simulation based teaching. In this work we investigate the effectiveness of a role of web based computer simulation teaching in electromagnetic induction [1, 2, 3].

II. METHOD

The student sample: Sample for this study included the 30 students of plane science of higher secondary level. All students are of same rank. Simulation based teaching is new thing for them [4, 5, 6].

Treatments: Theory based lecture on the faraday's law of electromagnetic induction and its applications was given to students for six hours; one hour daily for six days. Lecture contents are given in Appendix A. During lecture care was taken that on student should remain absent in any of six lectures. On the seventh day multiple choice question tests was taken to check their understanding of theory of EMI. Questions were selected from various section text books [7]. Test includes total 30 questions. It includes equal number of theory, conceptual, application based questions. Time allotted to each question is of 2 minutes. After test Question papers were collected back from students. Students response to this test is given in following table I and response is shown in the figure I

TABLE I. Student's response in the form of write and wrong answers before Faraday's simulation lab work

Question type	Answers given by all 30 students	
	Write answers	Wrong answers
Theory based	247	53
Concept based	198	102
Application based	168	132
Total Answers	613	287

FIGURE I.

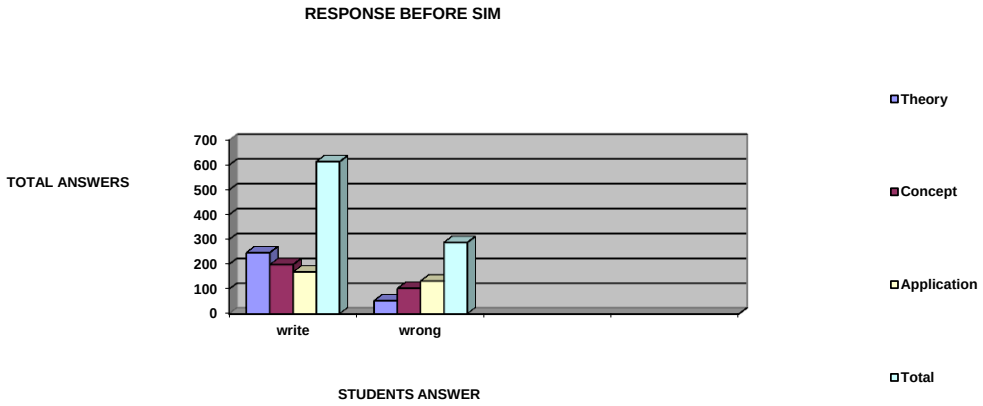

On the same day Faradays lab simulation is played on LCd projector in classroom. The information about each experiment of simulation was given to the students. Demonstration of every experiment was given to the students. After it students were divided into five groups and they were allowed to do the experiment with the faraday's lab simulation software in computer lab due to limited sources. Same multiple choice question test was again taken just after faradays lab simulation experiments. Now answers given by students were

evaluated and are given in following table II and response is shown in figure II.

TABLE II Students response in the form of write and wrong answers after Faraday's simulation lab work

Question type	Answers given by all 30 students	
	Write answers	Wrong answers
Theory based	290	10
Concept based	270	30
Application based	281	19
Total Answers	841	59

FIGURE II

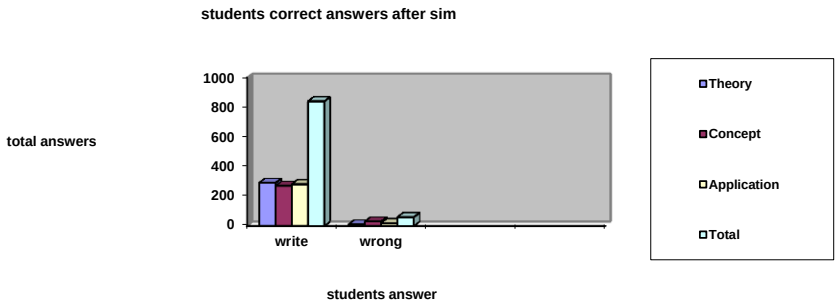

III. FARADAY'S EMI LAB SIMULATION EXPERIMENTS

Five experiments of EMI LAB SIM are performed by students using carefully design instructions. Snap shot of simulation is given in figure III.

Figure III Snap shot of Faraday's Lab Sim

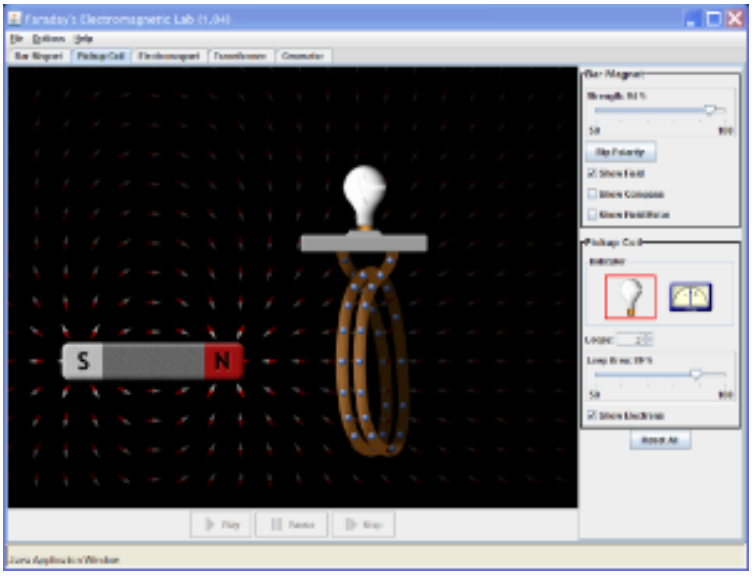

The experiments are;

III A Bar magnet; compass and field meter experiment: It describes the strength, direction of magnetic field of bar magnet at different positions near it. This part of simulation is related with the following equations

$$B = \frac{m}{4p}\frac{M}{r^3}\ \sqrt{3cos^2 q + 1}$$

and $\alpha = tan^{-1}\ \frac{1}{2}\ tan\theta$

Instructions

1. Here you will find a compass and a bar magnet. What do the two have in common?
2. Slowly move the compass around the bar magnet. What observations do you make? How can you explain what you are witnessing?
3. Increase and decrease the strength of the bar magnet (use slider) and continue to slowly move the compass around the bar magnet. What effect does changing the magnet's field strength appear to have on the compass?
4. Place the compass next to the South Pole of the bar magnet and press the Flip Polarity button. What happens to the magnet and the compass?
5. Click See Inside Magnet. What do you see?
6. Click Show Field Meter and move the meter around. In what position does B have the greatest magnitude? When does it get weaker?
7. Where is Bx positive? Where is it negative? Where is By positive? Where is it negative?
8. Place the meter at a location to the left and underneath the bar magnet. What are the Bx, By and B Values? Verify the mathematical relationship between the three.

IIIB. Bar magnet coil experiment: It describes the Lenz's Faraday's law of EMI. It describes the equation

$$e = -\frac{d\phi}{dt}$$

Instructions

1. Here you have a bar magnet and a coil of wire attached to an incandescent light bulb. Does the coil or the bar magnet appear to be creating the magnetic field? How can you verify this?
2. Click the Show Electrons box off and back on. What does it do, visually?
3. Move the bar magnet around the outside of the coil/bulb apparatus. What do you observe happening to the coil/bulb?
4. What could possibly explain WHY this is occurring?
5. Now, move the bar magnet back and forth inside the coil of wire. Thoroughly describe and explain your observations.
6. Increase and decrease the strength of the bar magnet (slider) and repeat. What effect does changing the magnet's strength have?
7. Set the bar magnet strength at 75% and continue to move the magnet. Decrease the number of loops to 1, and then increase it to 3. What effect does this have?
8. Replace the incandescent bulb with the Voltage meter and return loop # to 3. What happens when you move the bar magnet back-n-forth through the loop? Does this appear to be creating a Direct Current or an Alternating Current? How do you know?
9. What effect does changing the bar magnet strength or the number of loops seem to have on the voltage? What combination gives you the greatest?

IIIC Electromagnet experiment: It describes the Biot-Savart law and magnetic field produced by bar magnet. It is based upon the equation

$$\boxed{B = \mu_0 NI}$$

Instructions:

1. Here you will find a compass and a power supply (battery) connected to a coil of wire. What effect does the battery appear to be having on the wire?
2. How can you confirm that the battery is, indeed, a DC power supply…and not just trust the label by the picture?

3. What appears to be creating the magnetic field being represented here? How can moving the compass around confirm that?
Why do you suppose the magnetic field surrounding the compass is not being represented by the simulation in this instance?
4. Does changing the number of loops appear to have an effect on the rate of motion of the electrons in the wire? Explain.
5. Gradually decrease the voltage of the battery from 10 V to 5 V. What effects does that appear to have on things?
6. What happens when the voltage is 0 V?
7. You may have noticed that you can continue to slide the voltage bar to the left. What does that do? Explain. (Slide bar back-n-forth a couple times to confirm).
8. Press the Show Field Meter button. Set the voltage to 10 V. What is the strength of the magnetic field inside the coil?
9. Decrease the voltage to 5 V. What effect did that have on the field strength? What kind of relationship do the two appear to have?
10. Replace the battery with an AC Current Supply. What effect does this have on the wire, the compass and the magnetic field meter?

IIID. Transformer experiment: It is based upon principle of mutual induction and describes the following equations.

$$e_s = -M\frac{dI_p}{dt}$$

and

$$\frac{\boldsymbol{e_s}}{\boldsymbol{e_p}} = \frac{\boldsymbol{n_s}}{\boldsymbol{n_p}}$$

Instructions:

1. Connect the D.C. source in the first coil and fixed its voltage. Note whether emf get induced in the secondary coil or not. Change the d.c. voltage continuously and note its effect on emf induced in secondary coil.
2. Replace DC supply of primary coil by AC source. Change the amplitude, frequency of AC source and observe its effect on the emf induced in secondary coil.
3. Note the effect on induced emf if number of loops and area of secondary coil is changed

IIIE. AC generation experiment: In this simulation rotating bar magnet induces emf in the fixed coil. By changing the area, number of turns of coil and rotational speed of bar magnet student can change the magnitude of induce emf. It is based upon following equations.

$$e = -\frac{d}{dt}[n\,A\,B\cos(\omega t)]$$

Instructions:

1. Here you will find a water faucet, a compass, a bar magnet on a wheel (turbine), and a coil of wire connected to an incandescent bulb. Move the compass around a little and determine what it is reacting to at this time.
2. Turn the faucet on, just enough to get about 10 RPM on the turbine. What effect does this have on the compass and the wire/bulb?
3. Increase the rotation to about 20, 50, even 100 RPM. What effect does that appear to have on the compass, the wire and the bulb?
4. Increase and decrease the number of loops. What effect does this have?
5. Increase and decrease the bar magnet's strength. What effect does this have?
6. Replace the bulb with a Voltage Meter. What effect does increasing the RPMs have on the amount of voltage?
7. Does the rotating magnet appear to create a Direct or Alternating Current? Explain.
8. What effect does the number of loops appear to have on the voltage?
9. The moving of this magnet has created an electric current in the coil, which is being utilized by the bulb! Do you know what we call such a device? What is it?
10. If we could reverse this process, what would we call the device? What would one do to make that work? Can you get the simulation to do it?

Students can study the importance of each variable in every equation of EMI using above simulations and instructions.

IV. OUTCOMES OF THE STUDY

After faraday's simulation lab exercise students thinking and approach towards conceptual and application based question is changed. Maximum student had given correct answers to all questions which were not before. Response to theory based questions was near about same. This happens due to experiment performed by students using simulation. It is possible to do the experiment easily, without any risk only due to simulations. Experiments done by students had removed the understanding difficulties of the EMI theory.

V. CONCLUSIONS

Physics lab simulations are effective tools to describe each difficult concept of physics. Faraday's lab simulation is an easy way to enhance students understanding of faraday's theory of electromagnetic induction.

ACKNOWLEDGEMENTS

I am very thankful to organizer of PHET who had kept the simulations and made them freely available on their webpage. I am also thankful to Nicole Murawski of Royal Oak High School for his carefully designed instructions to use simulation effectively. I am also thankful to the head of my institute who had given active support for this work.

REFERENCES:

[1] McDermott, L. *How we teach and how students learn -a mismatch.* Am. J. phys. **61**, 295-298 (1993).

[2] Gokhale, A., *Effectiveness of computer simulation for enhancing higher order thinking.* Journal of Industrial Teacher Education **33**, 36-46 (1996).

[3] Choi, E., & Park, J., *Conditions for the effective use of*
simulations & its Applications to Middele-school physics inquiry activities, Journal of Korean Physical Society **42**, 318-324 (2003).

[4] Beerman, K., *Computer-based multimedia: new directions in teaching and learning*, Journal of Nutrition Education **28**, 15-18 (1996).

[5] *Magin, D. J. and Reizes, J. A., Computer simulation of laboratory experiments: An unrealized potential*. *Computers Educ*. **14**, 263-270 (1990)

[6] Tarekegn, G., *Can computer simulations substitute real laboratory apparatus?* Latin American Journal of Physics Education **3**, 506-517 (2009).

[7] NCERT Physics textbook for class XII ISBN 81-7450-631-4

APPENDIX A Lecture contents

1. Introduction of EMI phenomenon using Magnet-coil and coil-coil experiment
2. concept of Magnetic flux. Farady's law of EMI And problem of conservation of Energy.
3. Lenz's law of EMI.
4. Proof of Lenz's law of EMI.
5. Eddy current
6. Phenomenon of Self and Mutual induction. Concept of back emf.
7. Transformer construction; working and power losses.
8. AC generation by Rotating coil experiment

Physics Through Problem Solving - XXII
Quantum Mechanics Problems with Time-Evolution Operator

Ahmed Sayeed
Department of Physics
University of Pune
Pune - 411007
email: sayeed@physics.unipune.ac.in
(Dated: March 1, 2012)

In this article we solve some quantum mechanics problems using the time-evolution operator $U(t) = e^{-iHt/\hbar}$ for a time independent Hamiltonian H. We consider here the time evolution of a particularly simple system - a two-state system.

We learn in an introductory course in quantum mechanics that any physical system (an electron, an atom, a molecule etc.) has to be described by a state-vector $|\psi\rangle(t)$. The most familiar example of a state-vector is a wave-function, such as that of an electron in a hydrogen atom. We are also familiar with the state-vector that describes the spin state of a particle. The simplest example is the spin-state of a free electron (or any spin-1/2 particle). The state-vector $|\psi\rangle$ in this case is a column vector of size 2. If this state-vector is known we can calculate the probability of obtaining a result in any measurement on the system, such as, the measurement of energy or the spin component in a given direction. One of the basic tasks in quantum mechanics is to determine the state-vector of the system $|\psi(t)\rangle$ at a given instant of time t, given the the state-vector of the system $|\psi(0)\rangle$ at a given instant of time $t = 0$. One way of doing it is by solving the Schrödinger equation $i\hbar\frac{d|\psi(t)\rangle}{dt} = H|\psi(t)\rangle$. Another equivalent way of doing this is by using the time-evolution operator $U(t) = e^{-iHt/\hbar}$. This is physically more intuitive because you can think of the change in state-vector as caused by the action of an operator - you take $|\psi(0)\rangle$ and operate $U(t)$ on it, and you get $|\psi\rangle(t)$, that is, $U(t)|\psi(0)\rangle = |\psi(t)\rangle$. In the following problems we shall demonstrate this procedure.

The Hamiltonian for a two state system is given by (in the standard basis $\{|1\rangle, |2\rangle\}$)

$$H = \begin{pmatrix} E_0 & -\eta \\ -\eta & E_0 \end{pmatrix}$$

E_0 and η are not time-dependent.

Problem 1

Can E_0 and η be complex numbers?

Solution

The Hamiltonian is the operator for the observable energy. The operators representing observables have to Hermitian, that is to say, $H^\dagger = H$. Which is possible only if all the main-diagonal elements are real, and opposing off-diagonal elements are complex-conjugates of one another. In this case that means E_0 is real, and $(-\eta)^* = (-\eta) \implies \eta^* = \eta$, i.e. η is also real.

Problem 2

Find the eigenvalues and eigenvectors of H given in the previous problem.

Solution

The characteristic equation and the solutions are (λ is the eigenvalue)

$$|H - \lambda I| = 0 \implies (E_0 - \lambda)^2 - \eta^2 = 0 \implies \lambda = E_0 \pm \eta$$

where I is the 2×2 identity matrix. Let us call eigenvectors for the eigenvalues $E_1 = E_0 - \eta$ and $E_2 = E_0 + \eta$ respectively $|V_1\rangle$ and $|V_2\rangle$. We obtain the two eigenvectors by solving two eigenvalue equations $H|V_1\rangle = E_1|V_1\rangle$ and $H|V_2\rangle = E_2|V_2\rangle$. The first one is worked out as follows. Let $|V_1\rangle = \left(\begin{smallmatrix} x_1 \\ x_2 \end{smallmatrix}\right)$ and we have to determine x_1 and x_2.

$$\begin{pmatrix} E_0 & -\eta \\ -\eta & E_0 \end{pmatrix} \begin{pmatrix} x_1 \\ x_2 \end{pmatrix} = (E_0 - \eta) \begin{pmatrix} x_1 \\ x_2 \end{pmatrix}$$

which gives us two equations $E_0x_1 - \eta x_2 = (E_0 - \eta)x_1$ and $-\eta x_1 + E_0x_2 = (E_0 - \eta)x_2$. But these two equations are not independent - one can be obtained from the other. So we have one linear equation to determine two unknowns, which is impossible. But we can use this equation to determine the *ratio* of x_1 and x_2, and then apply normalization requirement to fix the values of x_1 and x_2.

Simplifying any one of the 'two' equations above we get $x_2 = x_1 = c$ say. Thus we have $|V_1\rangle = \left(\begin{smallmatrix} c \\ c \end{smallmatrix}\right)$. And c remains to be determined. But $|V_1\rangle$ is a quantum state of the system, and so must be normalized. Normalization gives us $c = 1/\sqrt{2}$. Thus we finally have $|V_1\rangle = \frac{1}{\sqrt{2}}\left(\begin{smallmatrix} 1 \\ 1 \end{smallmatrix}\right)$. Note that we can multiply this vector by a factor $e^{i\phi}$, where ϕ any real number, and it still remains normalized. Thus the quantum states we obtain are always uncertain within this *overall phase factor*. But it does not matter, because no measurable property of a system depends on the overall phase-factor of the state-vector. So for simplicity we usually set $\phi = 0$ so that the phase-factor is unity.

Working in the same way, the reader can easily find the second eigenvector as $|V_2\rangle = \frac{1}{\sqrt{2}}\left(\begin{smallmatrix} 1 \\ -1 \end{smallmatrix}\right)$. At this point it is important to do a check - we know that the eigenvectors of a Hermitian matrix, for distinct eigenvalues, are always mutually orthogonal. We can readily verify that the inner-products $\langle V_1|V_2\rangle$ and $\langle V_2|V_1\rangle$ are both zero and so everything is in order. One common practice in quantum mechanics is to label the eigenvectors of a matrix

by the respective eigenvalue. That is, we call $|V_1\rangle$ and $|V_2\rangle$ above $|E_1\rangle$ and $|E_2\rangle$. Thus the eigenvalue equations become simply $H|E_1\rangle = E_1|E_1\rangle$ and $H|E_1\rangle = E_1|E_1\rangle$. This can be slightly confusing for a beginner, but once you get used to it, it is very convenient when doing quantum mechanics linear algebra. We shall use this notation in the rest this article.

Problem 3

Consider a system described by the Hamiltonian H given in problem 1. At $t = 0$ the system is in the state

$$|\psi(0)\rangle = \frac{|1\rangle + i|2\rangle}{\sqrt{2}}$$

What are the probabilities that at time $t = 0$ the system is found in the states $|1\rangle$ and $|2\rangle$? What are the probabilities that the system is found in each of the two energy eigenstates?

Solution

Here $|1\rangle = \left(\begin{smallmatrix}1\\0\end{smallmatrix}\right)$ and $|2\rangle = \left(\begin{smallmatrix}0\\1\end{smallmatrix}\right)$ (i.e.,*standard basis vectors*). We know from one of the basic postulates of quantum mechanics that if at a given moment of time the system is in the state $|\psi\rangle$, the probability that an observation will find it in a state $|\phi\rangle$ is (assuming both the state vectors are normalized) $|\langle\phi|\psi\rangle|^2$. Thus the probability that at $t = 0$ the system is found in the state $|1\rangle$ is

$$\begin{aligned}|\langle 1|\psi(0)\rangle|^2 &= \left|\langle 1|\left[\frac{1}{\sqrt{2}}|1\rangle + \frac{i}{\sqrt{2}}|2\rangle\right]\right|^2 \\ &= \left|\frac{1}{\sqrt{2}}\left[\langle 1|1\rangle + i\langle 1|2\rangle\right]\right|^2 \\ &= \left|\frac{1}{\sqrt{2}}\left[1+0\right]\right|^2 \\ &= \frac{1}{2}\end{aligned}$$

We have used above the orthonormality of the basis vectors, i.e. $\langle 1|1\rangle = 1$ and $\langle 1|2\rangle = 0$. Similarly we get the probability that at $t = 0$ the system is found in the state $|2\rangle$ also $\frac{1}{2}$.

The probabilities for finding the system in energy eigenstates $|E_1\rangle$ and $|E_1\rangle$ are respectively $|\langle E_1|\psi(0)\rangle|^2$ and $|\langle E_2|\psi(0)\rangle|^2$. Let us first evaluate the components $\langle E_1|\psi(0)\rangle$ and $\langle E_2|\psi(0)\rangle$. We have

$$|E_1\rangle = \frac{1}{\sqrt{2}}\begin{pmatrix}1\\1\end{pmatrix} = \frac{1}{\sqrt{2}}\begin{pmatrix}1\\0\end{pmatrix} + \frac{1}{\sqrt{2}}\begin{pmatrix}0\\1\end{pmatrix} = \frac{1}{\sqrt{2}}|1\rangle + \frac{1}{\sqrt{2}}|2\rangle \tag{1}$$

And

$$|E_2\rangle = \frac{1}{\sqrt{2}}\begin{pmatrix}1\\1\end{pmatrix} = \frac{1}{\sqrt{2}}|1\rangle - \frac{1}{\sqrt{2}}|2\rangle \tag{2}$$

And we are given

$$|\psi(0)\rangle = \frac{1}{\sqrt{2}}|1\rangle + \frac{i}{\sqrt{2}}|1\rangle \tag{3}$$

From Eqs. (1) and (3) we get

$$\begin{aligned}\langle E_1|\psi(0)\rangle =& \langle E_1|\left[\frac{|1\rangle + i|2\rangle}{\sqrt{2}}\right] \\ =& \left[\langle 1|\frac{1}{\sqrt{2}} + \langle 2|\frac{1}{\sqrt{2}}\right]\left[\frac{|1\rangle + i|2\rangle}{\sqrt{2}}\right] \\ =& \frac{1}{2}\left[\langle 1|1\rangle + \langle 2|1\rangle + i\langle 1|2\rangle + i\langle 2|2\rangle\right] \\ =& \frac{1}{2}\left[1+i\right]\end{aligned} \tag{4}$$

And from Eqs. (2) and (3) we get

$$\begin{aligned}\langle E_2|\psi(0)\rangle =& \langle E_1|\left[\frac{|1\rangle + i|2\rangle}{\sqrt{2}}\right] \\ =& \frac{1}{2}\left[1-i\right]\end{aligned} \tag{5}$$

And from Eqs. (4) and (5) we immediately get $|\langle E_1|\psi(0)\rangle|^2 = \frac{1}{2}$ and $|\langle E_2|\psi(0)\rangle|^2 = \frac{1}{2}$.

Problem 4

Answer the questions in the previous problem for $t > 0$, using the time-evolution operator.

Solution

We begin by expanding the state vector $|\psi(0)\rangle$ in the $\{|E_1\rangle, |E_2\rangle\}$ basis:

$$|\psi(0)\rangle = |E_1\rangle\langle E_1|\psi(0)\rangle + |E_2\rangle\langle E_2|\psi(0)\rangle \tag{6}$$

Using Eqs (4) and (5) in Eq. (6) we get

$$|\psi(0)\rangle = \frac{1}{2}(1+i)|E_1\rangle + \frac{1}{2}(1-i)|E_2\rangle \tag{7}$$

In Eq. (7) we have expressed the state vector $|\psi(0)\rangle$ in the energy eigenbasis. Now we can operate the time-evolution operator for the time independent Hamiltonian, $U(t) = e^{-iHt/\hbar}$, on this state vector and obtain the state vector at time t, that is $|\psi(t)\rangle$:

$$\begin{aligned}|\psi(t)\rangle &= U(t)|\psi(0)\rangle \\ &= e^{-iHt/\hbar}|\psi(0)\rangle \\ &= e^{-iHt/\hbar}\left[\frac{1}{2}(1+i)|E_1\rangle + \frac{1}{2}(1-i)|E_2\rangle\right] \\ &= \left[\frac{1}{2}(1+i)e^{-iHt/\hbar}|E_1\rangle + \frac{1}{2}(1-i)e^{-iHt/\hbar}|E_2\rangle\right] \\ &= \left[\frac{1}{2}(1+i)e^{-iE_1t/\hbar}|E_1\rangle + \frac{1}{2}(1-i)e^{-iE_2t/\hbar}|E_2\rangle\right]\end{aligned} \tag{8}$$

In the last step we have used the fact that when the time-evolution operator $e^{-iHt/\hbar}$ (H being time-independent) acts on an energy eigenstate $|E\rangle$, the eigenstate gets multiplied by the factor $e^{-iEt/\hbar}$, E being the energy eigenvalue for the state. Note that $e^{-iEt/\hbar}$ is a number (or scalar).

We are now ready to calculate the probabilities that at time t, the system is in the states represented by vectors $|1\rangle$ and $|2\rangle$. The probability that at time t the system is found in the state $|1\rangle$ is :

$$\begin{aligned}P_1(t) &= |\langle 1|\psi(t)\rangle|^2 \\ &= \left|\langle 1|\left[\frac{1}{2}(1+i)e^{-iE_1t/\hbar}|E_1\rangle + \frac{1}{2}(1-i)e^{-iE_2t/\hbar}|E_2\rangle\right]\right|^2 \\ &= \left|\left[\frac{1}{2}(1+i)e^{-iE_1t/\hbar}\langle 1|E_1\rangle + \frac{1}{2}(1-i)e^{-iE_2t/\hbar}\langle 1|E_2\rangle\right]\right|^2\end{aligned}$$

From Eqs. (1) and (2) we have $\langle 1|E_1\rangle = \frac{1}{\sqrt{2}}$ and $\langle 1|E_2\rangle = \frac{1}{\sqrt{2}}$. Using this the last equation above we have

$$\begin{aligned}P_1(t) &= \left|\left[\frac{1}{2}(1+i)e^{-iE_1t/\hbar}\frac{1}{\sqrt{2}} + \frac{1}{2}(1-i)e^{-iE_2t/\hbar}\frac{1}{\sqrt{2}}\right]\right|^2 \\ &= \left(\frac{1}{2\sqrt{2}}\right)^2\left|\left[(1+i)e^{-iE_1t/\hbar} + (1-i)e^{-iE_2t/\hbar}\right]\right|^2 \\ &= \frac{1}{8}\left|\left[(1+i)e^{-iE_1t/\hbar} + (1-i)e^{-iE_2t/\hbar}\right]\right|^2\end{aligned}$$

We can simplify the modulus-squared term in the last expression above by noting that for a complex number z, $|z|^2 = zz^*$, and also $e^{i\theta} - e^{-i\theta} = 2i\sin\theta$. After a few lines of simplification, we get

$$\begin{aligned}P_1(t) &= \frac{1}{2}\left[1 - \sin\left(\frac{E_2 - E_1}{\hbar}t\right)\right] \\ &= \frac{1}{2}\left[1 - \sin\left(\frac{2\eta}{\hbar}t\right)\right]\end{aligned}$$

In the last line we have used $E_2 - E_1 = 2\eta$. An almost identical calculation gives the probability that at time t the system is found in the state $|2\rangle$:

$$\begin{aligned}P_2(t) &= |\langle 2|\psi(t)\rangle|^2 \\ &= \frac{1}{2}\left[1 + \sin\left(\frac{2\eta}{\hbar}t\right)\right]\end{aligned}$$

Note that the two probabilities add to 1. This is because this is a two-state system, and the states $|1\rangle$ and $|2\rangle$ are mutually orthogonal. Thus is the system in not one state, it must be in the other.

Similarly, the probability that at time t the system is found in the energy eigenstate E_1 is given by $|\langle E_1|\psi(t)|^2$. This we can calculate by using Eq. (1) in (8):

$$\begin{aligned}P(t, E = E_1) &= |\langle E_1|\psi(t)\rangle|^2 \\ &= \left|\langle E_1|\left[\frac{1}{2}(1+i)e^{-iE_1t/\hbar}|E_1\rangle + \frac{1}{2}(1-i)e^{-iE_2t/\hbar}|E_2\rangle\right]\right|^2 \\ &= \left|\left[\frac{1}{2}(1+i)e^{-iE_1t/\hbar}\langle E_1|E_1\rangle + \frac{1}{2}(1-i)e^{-iE_2t/\hbar}\langle E_1|E_2\rangle\right]\right|^2 \\ &= \left|\left[\frac{1}{2}(1+i)e^{-iE_1t/\hbar} + 0\right]\right|^2 \\ &= \frac{1}{2}\end{aligned}$$

In the above we have used the orthonormality of $|E_1\rangle$ and $|E_2\rangle$ (i.e. $\langle E_1|E_1\rangle = 1$, $\langle E_1|E_2\rangle = 0$) and $|e^{-iE_1t/\hbar}|^2 = 1$.

In the same manner we get

$$
\begin{aligned}
P(t, E = E_2) &= |\langle E_2|\psi(t)\rangle|^2 \\
&= \left|\langle E_2| \left[\frac{1}{2}(1+i)e^{-iE_1 t/\hbar}|E_1\rangle + \frac{1}{2}(1-i)e^{-iE_2 t/\hbar}|E_2\rangle\right]\right|^2 \\
&= \left|\left[\frac{1}{2}(1+i)e^{-iE_1 t/\hbar}\langle E_2|E_1\rangle + \frac{1}{2}(1-i)e^{-iE_2 t/\hbar}\langle E_2|E_2\rangle\right]\right|^2 \\
&= \left|\left[0 + \frac{1}{2}(1+i)e^{-iE_2 t/\hbar}\right]\right|^2 \\
&= \frac{1}{2}
\end{aligned}
$$

Once again the two probabilities add up to 1, for the same reason - the states $|E_1\rangle$ and $|E_2\rangle$ are mutually orthogonal for a two-state system. Note that the probabilities of finding the system in an energy eigenstates is *independent of time*, that is, they are same as at time $t = 0$, as we have seen in the previous problem. This is true in general when the Hamiltonian is time independent. But we have also seen that the probabilities of finding the system in some arbitrary state, such as $|1\rangle$ and $|2\rangle$ considered above, in general vary with time.

Ground states of continuum models

Oscar Bolina
Kaplan Shinyway Overseas Pathway College,
337 Zhishan Road, Binjiang District, HangZhou 310053

(*Submitted December 6, 2009*)

Abstract

We calculate the ground state energies of a system of electrons in one-dimensional infinitely deep square well potentials. We analyze the cases when the wells are regularly spaced and when they are clustered together to form one single large well. These potentials are intended to physically describe the interaction of electrons and nuclei in a continuum model. We investigate which potential yields the minimum ground state energy using elements of interpolation potential in quantum mechanics derived from first principles. We also mention models of crystalline formation that are related to this problem.

PACS { 73.21.Fg, 73.22 Dj

Ground states of continuum models

Oscar Bolina

Kaplan Shinyway Overseas Pathway College,

337 Zhishan Road, Binjiang District, HangZhou 310053

(Dated: July 2, 2009)

We calculate the ground state energies of a system of electrons in one-dimensional infinitely deep square well potentials. We analyze the cases when the wells are regularly spaced and when they are clustered together to form one single large well. These potentials are intended to physically describe the interaction of electrons and nuclei in a continuum model. We investigate which potential yields the minimum ground state energy using elements of interpolation potential in quantum mechanics derived from first principles. We also mention models of crystalline formation that are related to this problem.

PACS – 73.21.Fg, 73.22 Dj

I. INTRODUCTION

We study a system of electrons in infinitely deep square well potentials in two situations. In the first situation the potential consists of M regularly spaced wells, each of them having the form

$$V_{\rm r}(x) = \begin{cases} 0 & \text{for} \quad (j-1)(b+a) \leq \ x \ \leq j(b+a)-a \\ \infty & \text{for} \quad x=(j-1)(b+a) \ \text{ and } \ x=j(b+a)-a \end{cases} \tag{1}$$

for $j = 1, 2, 3, ..., M$.

In the second situation, the M wells are all clustered together forming one single large well. The corresponding potential is

$$V_{\rm c}(x) = \begin{cases} 0 & \text{for} \quad 0 < \ x \ < M(b+a)-a \\ \infty & \text{for} \quad x=0 \ \text{ and } \ x=M(b+a)-a. \end{cases} \tag{2}$$

The potential (1) is intended to represent electrons bound to individual nuclei arranged in an orderly pattern, whereas potential (2) is intended to represent electrons bound to the set of nuclei.

We are interested in the ground state of a system of N electrons in potentials (1) and (2), and we would like

to compare the ground state energies in these potentials in order to determine whether the lowest ground state energy corresponds to the configuration of potential (1) or of potential (1). The ordered arrangement of potential (1) is interpreted as corresponding to crystallization or existence of a period ground state.

This is a very simplified version of a much broader problem of understanding crystallization in continuum models and of determining whether crystallization is in any way induced by the discrete character of the lattice models in which this phenomenon has been observed[1],[2]. At low temperatures, matter displays a crystalline structure. The particles of matter are arranged in an orderly pattern that is repeated throughout the material. This arrangement is associated with a minimum energy of the system.

One of the lattice model of crystalline formation is the Falicov-Kimball model. This a lattice model in which ions are fixed at the lattice sites and spinless electrons move about and interact with the ions only when they both happen occupy the same site. There is no interaction between electrons. For certain values of the ion-electron interaction and for certain values of the number of particles present, the ions display a checkerboard pattern in the ground state of the model. This regular configuration of the ions is associated with the existence of periodic ground states. See[3] for details and further results on this model.

In the present case, the question is immediately raised whether it is legitimate to compare ground state energies for two *different* potentials. It is clear that if we consider two energy states for the `same` potential then the state with lower energy is the ground state. We show that the comparison of ground state energies in this case is meaningful. The key ingredient is a varying parameter that will provide a transition from potential of Eq. (2) to that of Eq. (1) thus allowing for the comparison of ground state energies. This is carried out in section II.

Next in section III we find that the ground state energy for potential (1) is always `higher` than that for potential (2) and hence the minimum ground state energy does not correspond to the arrangement of electrons in potential (1).

II. THE INTERPOLATION POTENTIAL

The comparison of energies for the different potentials of Eqs. (1) and (2) is meaningful because the potential V_h shown in Fig. 1 interpolates between these two cases, with $h \to \infty$ being potential (1) and $h \to 0$ being potential (2).

For electrons on an interval $[p, q]$, let $\mathcal{H}_{[p,q]}$ be the Hilbert space of single-electron states. For `spinless` electrons, $\mathcal{H}_{[p,q]} = L^2([p, q], dx)$. It follows that for finite h single-electron states under the potential of Fig 1 lie on $\mathcal{H}_{[0,2b+a]} = L^2([0, 2b + a], dx)$, and a vector state of a system of N electrons will lie on the closed

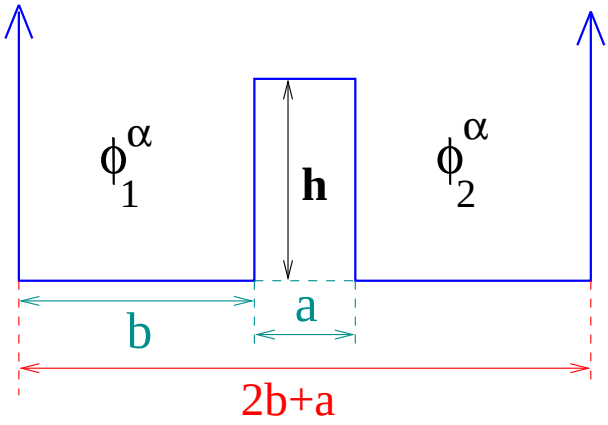

FIG. 1: This potential interpolates between potentials of Eqs. (1) and (2) when $M = 2$ as the height h is sent to infinity or zero respectively.

antisymmetric subspace $\mathcal{H}^N_{[0,2b+a]}$ of

$$\mathcal{H}^N_{[0,2b+a]} = \underbrace{\mathcal{H}_{[0,2b+a]} \otimes \cdots \otimes \mathcal{H}_{[0,2b+a]}}_{N \text{ times}} .$$

For N normalized single-electron states $\Psi_h^{\alpha_\nu} \in \mathcal{H}_{[0,2b+a]}$ for $\nu = 1, 2, \ldots, N$ the anti-symmetrization operator $\mathcal{A}$ is given by

$$\mathcal{A}\left(\Psi_h^{\alpha_1} \otimes \cdots \otimes \Psi_h^{\alpha_N}\right) = \frac{1}{\sqrt{N}} \sum_{\pi \in S_N} \epsilon_\pi \Psi_h^{\alpha_{\pi(1)}} \otimes \cdots \otimes \Psi_h^{\alpha_{\pi(1)}} , \tag{3}$$

where S_N is the permutation group of N elements and ϵ_π equals ± 1 according to the parity of π. In coordinate space the wave-function for a system of N electrons is given by the well-known Slater determinant

$$\Psi_h^\alpha(x_1, \ldots, x_N) = \frac{1}{\sqrt{N}} \sum_{\pi \in S_N} \epsilon_\pi \Psi_h^{\alpha_{\pi(1)}}(x_1) \otimes \cdots \otimes \Psi_h^{\alpha_{\pi(1)}}(x_N) . \tag{4}$$

If H_h^N is the Hamiltonian of N non-interacting electrons under the potential of Fig. 1, then H_h^N acts in the antisymmetric subspace $H^N_{[0,\,2b+a]}$ as

$$H_h^N = \sum_{\nu=1}^{N} \underbrace{\mathbb{1} \otimes \cdots \otimes \mathbb{1}}_{\nu-1 \text{ times}} \otimes H_h \otimes \underbrace{\mathbb{1} \otimes \cdots \otimes \mathbb{1}}_{N-\nu \text{ times}} ,$$

where H_h is the single-electron Hamiltonian (without spin interactions)

$$H_h = -\frac{\hbar^2}{2\mu}\nabla^2 + V_h , \tag{5}$$

acting on $\mathcal{H}_{[0,\,2b+a]}$, with μ being the mass of the electron.

What happens now when the limit $h \longrightarrow \infty$ is taken? If $\Psi_h^\alpha \in \mathcal{H}_{[0,\,2b+a]}$ is a normalized wave-function of a single electron under the potential V_h of Fig. 1 then, when $h \to \infty$, due to exponential damping of Ψ_h^α on the interval $[b, b+a]$, one has

$$\Psi_h^\alpha \;\stackrel{h\to\infty}{\longrightarrow}\; c_1\phi_1^\alpha + c_2\phi_2^\alpha \tag{6}$$

where ϕ_i^α for $i = 1, 2$ are the normalized wave-functions defined in each of the potential wells obtained from Fig. 1 after h goes to infinity.

According to our notation ϕ_1^α lies on $\mathcal{H}_{[0,\,b]}$ and ϕ_2^α lies on $\mathcal{H}_{[b+a,\,2b+a]}$. Due to the normalization condition in (6), the coefficients satisfy $|c_1^\alpha|^2 + |c_2^\alpha|^2 = 1$. According to our notation, ϕ_1^α lies on $\mathcal{H}_{[0,b]}$ and ϕ_2^α lies on $\mathcal{H}_{[b,2b+a]}$. Both $\mathcal{H}_{[0,b]}$ and $\mathcal{H}_{[b,2b+a]}$ are closed orthogonal subspaces of $\mathcal{H}_{[0,2b+a]}$ and the sums in (6) can be interpreted as direct sums.

On the other hand, the single-electron Hamiltonian H_h in (5) converges, in the limit $h \longrightarrow \infty$, to a direct sum $\mathcal{H}_h = H_1 + H_2$ acting on $\mathcal{H}_{[0,b]} \oplus \mathcal{H}_{[b,2b+a]}$, where H_1 and H_2 are the single-electron Hamiltonians $-\frac{\hbar^2}{2\mu}\frac{d^2}{dx^2}$ restricted, respectively, to the intervals $[0, b]$ and $[b, 2b+a]$.

The crucial observation to make is that if Ψ_h^α are normalized eigenstates of H_h, i.e. $H_h\Psi_h^\alpha = E_h^\alpha\Psi_h^\alpha$, then it is not necessarily true that the states ϕ_i^α in (6) are eigenstates of H_i. However, due to the exponential damping of Ψ_h^α on the interval $[b, b+a]$ that, in the limit $h \longrightarrow \infty$,

$$E_h^\alpha = (\Psi_h^\alpha, H_h\Psi_h^\alpha) \;\longrightarrow\; |c_1^\alpha|^2\,(\phi_1^\alpha H_1\phi_1^\alpha) + |c_2^\alpha|^2\,(\phi_2^\alpha H_2\phi_2^\alpha)\,, \tag{7}$$

where the right-hand side above is a convex linear combination of the expectation values $(\phi_1^\alpha H_1\phi_1^\alpha)$ and $(\phi_2^\alpha H_2\phi_2^\alpha)$.

It now follows that in the resulting symmetric potential of Fig. 1 obtained after taking the limit $h \longrightarrow \infty$ we have $E_1^\alpha = (\phi_1^\alpha H_1\phi_1^\alpha) = E_2^\alpha = (\phi_2^\alpha H_2\phi_2^\alpha) = E^\alpha$, so that

$$E_h^\alpha = (\Psi_h^\alpha, H_h\Psi_h^\alpha) \longrightarrow (\phi_i^\alpha H_i\phi_i^\alpha) = E^\alpha. \tag{8}$$

For the case of multi-particle states $\mathcal{A}\,(\Psi_h^{\alpha_1} \otimes \cdots \otimes \Psi_h^{\alpha_N})$, with $\Psi_h^{\alpha_\nu}$ being eigenstates of H_h, the total energy is $\sum_{\nu=1}^N E_h^{\alpha_\nu}$. In this case, (7) now converges, as $h \to \infty$, to

$$\sum_{\nu=1}^N E_h^{\alpha_\nu} \;\longrightarrow\; \sum_{\nu=1}^N \Big[\,|c_1^{\alpha_\nu}|^2\,(\phi_1^{\alpha_\nu},\; H_1\phi_1^{\alpha_\nu}) + |c_2^{\alpha_\nu}|^2\,(\phi_2^{\alpha_\nu},\; H_2\phi_2^{\alpha_\nu})\Big]\,.$$

The same observations made above about ϕ_i^α being eigenstates and the fact that the resulting potentials are symmetric now lead, when $h \to \infty$, to

$$E_h^\alpha = \sum_{\nu=1}^N E_h^{\alpha_\nu} \;\longrightarrow\; \sum_{\nu=1}^N (\phi_1^{\alpha_\nu},\; H_1\phi_1^{\alpha_\nu}) = \sum_{\nu=1}^N E^{\alpha_\nu}\,. \tag{9}$$

The results (8) and (9) allow us to obtain a `lower` bound to E_h^α by taking respectively the minimum value of E^α and E^{α_ν} in these expressions. The important point is that the minimum value of the right-hand side of (9) is exactly the energy of the system of electrons which is obtained by successively filling up the single-electron energy levels of potential of Eq. (1) from the lowest levels up in each infinite well (Section III).

This lower bound to the energy of the system of electrons for the potential of Eq. (1) will be compared with an `upper` bound to the energy of the system of electrons for the potential of Eq. (2) (the case $h = 0$) to show that the energy of the electrons is minimized for the potential V_c. Since the parameter h provides a smooth transition from the potential of Eq. (1) to the potential of Eq. (2) when it varies from zero to infinity, we are justified in comparing system energies in the two different potentials.

III. THE GROUND STATE ENERGIES

The corresponding single-electron energies for the potential Eq. (1) are given by[4]

$$e_{\rm r} = \Big(\frac{\pi}{kb}\Big)^2 q^2 \tag{10}$$

for $q = 1, 2, 3, \ldots$, where b is the length of each well, $k^2 = 2\mu/\hbar^2$, and μ is the mass of the electrons. The ground state energy of a system of N electrons in potential (1) is the sum of the lowest energies in Eq. (10) in each well. In this case, it is convenient to write the total number of electrons as $N = nM + m$ for integers n and m, where m ($m < M$) is the remaining number of electrons after each of the M wells have been filled with n electrons.

The ground state energy is then

$$E_{\rm r} = \Big(\frac{\pi}{kb}\Big)^2 \Big[M\Big(\frac{n^3}{3} + \frac{n^2}{2} + \frac{n}{6}\Big) + m(n+1)^2\Big]. \tag{11}$$

Eq. (11) says that after n electrons have been distributed in the M wells, each of the remaining m electrons will be placed on the next higher energy level.

The single-electron energies for the potential of Eq. (2) admit upper bounds given by

$$e_{\rm c} = \Big(\frac{\pi}{Mkb}\Big)^2 q^2 \tag{12}$$

for $q = 1, 2, 3, \ldots$.

The ground state energy of a system of N electrons is again the sum of the successive lowest energies in

Eq. (12). We obtain

$$E_{\rm c} = \sum e_{\rm c} = \Big(\frac{\pi}{Mkb}\Big)^2 \Big(\frac{N^3}{3} + \frac{N^2}{2} + \frac{N}{6}\Big). \tag{13}$$

By substituting $N = nM + m$ into the above equation, we write

$$E_{\rm c} = \Big(\frac{\pi}{kb}\Big)^2 \left\{ \frac{M}{3} n^3 + \frac{2m+1}{2} n^2 + \frac{1 + 6m + 6m^2}{6M} n + \frac{m + 3m^2 + 2m^3}{6M^2} \right\}.$$

To compare the ground state energies, we calculate $\Delta E = E_{\rm r} - E_{\rm c}$ and obtain

$$\begin{aligned} \Delta E &= \Big(\frac{\pi}{kb}\Big)^2 \Big[M\Big(\frac{n^3}{3} + \frac{n^2}{2} + \frac{n}{6}\Big) + m(n+1)^2 \Big] - \Big(\frac{\pi}{Mkb}\Big)^2 \Big(\frac{N^3}{3} + \frac{N^2}{2} + \frac{N}{6}\Big) \\ &= \Big(\frac{\pi}{kb}\Big)^2 (xn^2 + yn + z), \end{aligned} \tag{14}$$

where

$$x = \frac{1}{2}(M-1)$$

is always positive for $M > 1$,

$$y = \frac{M}{6} + 2m - \frac{m^2}{M} - \frac{m}{M} - \frac{1}{6M} = \frac{M^2 + 6m(M-1) + 6m(M-m) - 1}{6M} > 0$$

under the conditions $M > 1$ and $m < M$, and

$$z = m - \frac{m + 3m^2 + 2m^3}{6M^2} = \frac{6mM^2 - (2m^3 + 3m^2 + m)}{6M^2} > \frac{m\,(M^2 - m^2)}{M^2} > 0$$

for $M > 1$ and $m < M$.

We thus conclude that ΔE in Eq. (14) is a positive quantity and the energy of the system for Eq. (2) is always lower than for Eq. (1) for all values of the parameters n, M and m under the given conditions of the problem.

The potentials studied here are of course too simple to answer the fundamental question of crystallization in continuum models. Important interactions have been left out (this is also true of more elaborate models as the Falicov-Kimball model). But they do allow for a definite answer to the problem posed within the simplified assumptions made.

Acknowledgments

It is a pleasure to thank Bruno Nachtergaele and João C. A. Barata.

---

[1] C. Radin, *Low temperature and the origin of crystalline symmetry*, Int. J. Mod. Phys. B **1** (1987) 1157-1191.

[2] R. J. Bursill, *One-dimensional continuum Falicov-Kimball model in the strongly correlated limit*, Physica A **206** 521–543 (1994).

[3] C. Gruber and N. Macris, *The Falicov-Kimball model: A review of exact results and extensions*, Helv. Phys. Acta **69**, 851–907 (1996).

[4] P. Landshoff and A. Metherell, *Simple Quantum Physics* (Cambridge University Press, Cambridge (1979) chapter 10.

Exact Eigenstates of a Relativistic Spin less Charged Particle in a Homogeneous Magnetic Field

T. Shivalingaswamy* and B.A. Kagali **
*Dept. of Physics, Govt College for Women, Mandya-571401, India.
tssphy@gmail.com
**Dept. of Physics, Bangalore University, Bangalore- 560056, India.
bakagali@gmail.com
(*Submitted* on 26/3/2011)

Abstract

Abstract: In this article we work out the exact eigenvalues and eigenfunctions of a spin less charged particle placed in a uniform magnetic field that has azimuthal symmetry. The possible applications are mentioned.

PACS: 03.65.Ge Keywords: Bound states; Landau Levels; Uniform Magnetic field

1. Introduction

In non-relativistic quantum mechanics, for a spin less charged particle placed in a uniform magnetic field, one obtains the well-known Landau-levels [1]. There are several applications of that result [2]. In many instances, charged particles can have relativistic high velocities [3], necessitating relativistic correct expressions for Landau-levels. In this article we deal with a relativistic spin less charged particle placed in a uniform magnetic field. We work out the exact energy eigenvalues and eigenfunctions. The formulae reproduce the Landau levels in the non-relativistic limit, as they should. Our result can find applications in astronomical bodies like white dwarfs and neutron stars.

Klein-Gordon particle in a uniform magnetic field

The modern theory of interaction of fields and particles demands the exact solutions that describe the quantum states of charged spin less particles in the external electromagnetic fields. Such solutions are very much useful to analyze and characterize these particles in the external fields.

The relativistic relation that connects energy and momentum of a free particle is given by

$$E^2 = P^2c^2 + m^2c^4$$

where E includes rest mass energy mc^2.
Replacing E and P by their corresponding operators

$$E \rightarrow i\hbar\frac{\partial}{\partial t}$$

and

$$P \longrightarrow -i\hbar\,\nabla$$

and then operating on a wave function $\psi(\boldsymbol{r}, t)$, we get

$$-\hbar^2\frac{\partial^2\psi}{\partial t^2} = -\hbar^2c^2\vec{\nabla}^2\psi + m^2c^4\psi \qquad (1)$$

The above equation is the well known Klein-Gordon equation for a free particle. The Klein-Gordon equation for a charged spin less particle placed in an electromagnetic field with potentials $\left(\phi, \frac{\vec{A}}{c}\right)$ is obtained by using the minimum coupling rule [4] as:

$$\left[i\hbar\frac{\partial}{\partial t}-e\phi\right]^2\psi(\vec{r},t)=\left(-i\hbar c\vec{\nabla}-e\vec{A}\right)^2\psi(\vec{r},t)+m^2c^4\psi(\vec{r},t)$$

in the transmitted light composed of multiple degrees of elliptical polarization.

For a uniform magnetic field *H*, which is chosen to be along *z* direction, we can choose the potentials as:

$$\phi=0,\ H_x=H_y=0,\quad A_z=0,\ A_x=-\frac{yH}{2},\ A_y=\frac{xH}{2} \tag{3}$$

For a static magnetic field,

$$\text{div}\,\vec{A}=0$$

Thus for a time-independent magnetic field the energy eigenvalues and eigenfunctions may be obtained by solving the following equation: For two space dimensions,

$$E^2\psi(\vec{r})=\left[-\hbar^2c^2\nabla^2-eHcL_z+\frac{e^2H^2}{4}\left(x^2+y^2\right)+m^2c^4\right]\psi(\vec{r}) \tag{4}$$

In terms of cylindrical coordinates $(\vec{r},\phi,z)$ this equation simplifies to

$$E^2\psi(\vec{r},\phi,z)=-\hbar^2c^2\left[\frac{1}{r}\frac{\partial}{\partial r}\left(r\frac{\partial}{\partial r}\right)+\frac{1}{r^2}\frac{\partial^2}{\partial\phi^2}+\frac{\partial^2}{\partial z^2}\right]\psi(\vec{r},\phi,z)+ieHc\,\hbar\frac{\partial}{\partial\phi}\psi(\vec{r},\phi,z)$$
$$+\frac{e^2H^2}{4}r^2\psi(\vec{r},\phi,z)+m^2c^4\psi(\vec{r},\phi,z)$$

This equation could be solved by the method of separation of variables using ansatz

$$\psi(\vec{r},\phi,z)=R(r)\Phi(\phi)Z(z) \tag{6}$$

Taking $\Phi\sim e^{il\phi}$ and $Z(z)\sim e^{ikz}$,

clearly the motion along the *z*-direction, the direction of the magnetic field is that of a free particle. For simplicity, we can put k = *0* without any loss of generality when we are considering the bound states.

The equations for $\Phi(\phi)$ and $R(r)$ will be:

$$\frac{d^2\Phi}{d\phi^2}=-l^2\Phi \tag{7}$$

$$\left[\frac{d^2}{dr^2}+\frac{1}{r}\frac{d}{dr}\right]R(r)+\left[\frac{E^2-m^2c^4}{\hbar^2c^2}-\frac{l^2}{r^2}-a^2r^2+2al\right]R(r)=0 \tag{8}$$

where

$$a=\frac{eH}{2\hbar c} \tag{9}$$

l has to be an integer due to periodic boundary condition $\Phi(\phi)=\Phi(\phi+2\pi)$. The radial equation can be reduced to the following convenient dimension less form by substitution $\rho=ar^2$

$$\left[\rho\frac{d^2}{d\rho^2}+\frac{d}{d\rho}+\left(\lambda+\frac{l}{2}\right)-\frac{\rho}{4}-\frac{l^2}{4\rho}\right]R=0 \tag{10}$$

Where $\lambda=\dfrac{E^2-m^2c^4}{4a\hbar^2c^2}$ (11)

Using the asymptotic conditions of the radial function

For large ρ equation (10) reduces to

$$\frac{d^2R}{d\rho^2}-\frac{1}{4}R\cong 0$$

$$R_{\pm} \sim e^{\pm\frac{\rho}{2}}$$

Only the negative power is acceptable from physical considerations.

For small ρ equation (10) reduces to

$$\frac{d^2R}{d\rho^2}+\frac{1}{\rho}\frac{dR}{d\rho}-\frac{l^2}{4\rho^2}R\cong 0 \qquad (12)$$

Taking $R \sim r^q$, we find for q the following equation:

$$q^2-\frac{l^2}{4}\cong 0$$

Hence

$$q=\pm\frac{l}{2} \qquad (13)$$

Once again, from physical considerations only $q=\frac{l}{2}$ is acceptable.

Hence putting

$$R(\rho)=\rho^{1/2}e^{-\rho/2}L(\rho)$$

We obtain the following equation for $L(\rho)$:

$$\rho\frac{d^2L}{d\rho^2}+[(l+1)-\rho]\frac{dL}{d\rho}+\left[\lambda+l-\frac{1}{2}\right]L=0 \qquad (14)$$

Power series solution of the following type for the above equation can be obtained:

$$L(\rho)=\sum_{\nu=0}^{\infty}a_\nu\rho^\nu \qquad (15)$$

The coefficients a_ν satisfy the following recurrence relation

$$a_{\nu+1}=\frac{\left(\nu+\frac{1}{2}-l-\lambda\right)}{(\nu+1)(\nu+l+1)}a_\nu \qquad (16)$$

Unless the power series terminates for some finite value of ν we get a diverging solution for *R (ρ),* similar to the solution obtained for the Hydrogen atom problem.

Let the highest value of ν that terminates the series be s, then

$$\lambda=\left(s-l+\frac{1}{2}\right) \qquad (17)$$

Putting

$$s - l = n \qquad (18)$$

We get

$$\lambda = (n+1/2) \qquad (19)$$

Where n is a positive integer.

Substituting for λ from equation (11), we find the allowed energy eigenvalues as:

$$E_n=\left[m^2c^4+2e\hbar cH\left(n+\frac{1}{2}\right)\right]^{\frac{1}{2}} \qquad (20)$$

These are the quantized energies of the charged particle.

We may expand the expression for energy in powers of $\frac{\hbar\Omega}{mc^2}$, where $\Omega=\frac{eH}{mc}$ is the cyclotron frequency in the magnetic field.

results have a good agreement with the theoretical predictions based on Eq. (1).

Then

$$E_n=mc^2+\hbar\Omega\left(n+\frac{1}{2}\right)-\frac{1}{2}\frac{\hbar^2\Omega^2}{mc^2}\left(n+\frac{1}{2}\right)^2+.... \qquad (21)$$

While the first term is the rest energy, the second term is precisely the non- relativistic Landau term. The third term may be taken as the relativistic correction to the Landau energy levels.

The normalized eigenfunctions may be expressed as:

$$\psi(\vec{r},\phi,z)=C_{nl}\left(ar^2\right)^{\frac{1}{2}}e^{-\frac{ar^2}{2}}L^l_{n+2l}\left(ar^2\right)e^{il\phi} \qquad (22)$$

Results and discussion

We have obtained exact expressions for the

energy eigenvalues and eigenfunctions for a relativistic spin less particle in a magnetic field. It is possible to apply our results to high-speed charged particles orbiting such astronomical bodies like white dwarfs and neutron stars. Our results may find use in understanding degeneracy [5] of particles of matter under relativistic conditions.

References:

[1] Pokrovsky V. L. (2009), *Modern Physics*, Physics-Uspekhi, **52**, 1169-1176.

[2] Tesanovic Z. and Sacramento P. D. (1998), *Landau levels and Quasiparticle spectrum of Landau levels of extreme type-II super-conductors*, Phys. Rev. Letters, **80,** 1521-1524.

[3] Hyman A. T. (1997), *Relativistic charged particle motion in a constant field according to Lorentz force law*, **65**, 195-198.

[4] Hoagland H. (1978), *Minimal electromagnetic coupling in elementary quantum mechanics,* J. Phys. A: Math. Gen. **11.**

[5] Kippenhahn R. and Weigert A. (1994), *Stellar structure and evolution*, Springer-verlag, First edition.

PC and digital camera assisted study of projectile motion

Yajun Wei Lijun Cui

A-level Center Affiliated to Nanjing University, 210093, Nanjing, China

(*Submitted* on 16/07/2011)

Abstract

We present a projectile motion experiment with the help of digital camera and PC for data acquisition and processing. In this experiment to study projectile motion with water stream, a photo of the water path is taken and the pixels coordinate of the photo is obtained to measure the length. This method is more effective and accurate than the traditional method. The experiment presents the idea of using digital camera and PC to measure distance and inspires students to look for new methods to solve problems.

1. Introduction

Water stream is commonly used for demonstrating trajectory of projectile motion in introductory-level physics [1-2]. If the trajectory of a horizontal projectile is known, the free fall acceleration can be determined. This is also a method to measure free fall acceleration. The common way to experimentally determine the trajectory in school laboratories is to draw the water path on a piece of paper and measure the lengths using a ruler [2]. This method can impose big subjective errors and complexity in operation when drawing the water path. We employ a digital camera and a computer (PC) to perform this task more effectively and accurately. A photo of the water path is taken. One pixel on the photo represents a certain length. We then get the lengths by reading the pixels directly. The experiment presents the idea of using digital camera and PC to measure distance and inspires students to look for new methods to solve problems.

The motion of a water drop is given by the equations below

$$x = vt \qquad (1)$$

$$y = \frac{1}{2}\, gi^2 \qquad (2)$$

where x and y are the displacements of the water drop along horizontal and vertical directions respectively (thus the coordinate of the trajectory), v is the initial speed of the water flow, g is the free fall acceleration and t is the time taken. By canceling t in eq, the equation for the trajectory is obtained to be

$$y = \frac{g}{2v^2}\, x^2 \qquad (3)$$

Once the trajectory and the initial speed of the water fall are measured, the value of g can then be calculated. The traditional way to decide a few sets of (x, y) values in school laboratories is to draw the water path on a piece of paper and measure the lengths using a ruler. This method can impose big subjective errors when drawing the water path. We employ a digital camera and a PC to perform this task and to process data. A picture of the water path can be taken using the camera (Fig 1). Any simple image-processing application

(e g. *Painter*) can be used to determine the pixel coordinates ( ) directly, as shown in Fig 2.

Fig 1. Recorded water path trajectory while demonstrating in a physics class

.

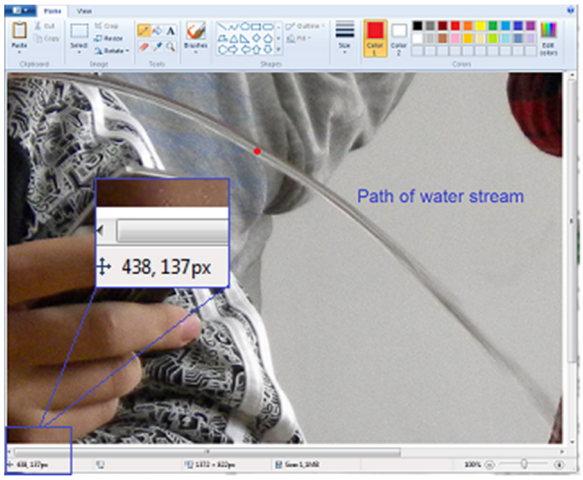

Putting a ruler or something of known length (a credit card 85.6mm long in our case) in the plane of the water path and counting the number of pixels the side length occupies on the photo, the length represented by each pixel a is obtained. Then,

$$x = n_x a, \quad y = n_y a \qquad (4)$$

Substituting eq. (4) into eq (3) yields,

—

Take a few data points from the water stream image, whose pixel coordinates can be directly read from the image processing application(for the case of Painter, it is in the bottom of the screen, as shown in Fig 2), and plot graph using MS Office Excel. Then the slope of the graph is $\frac{ga}{2v^2}$. The graph for our experiment is shown in Fig 3. We can see that the graph can be well fitted to a straight line, which indicates that the trajectory of a projectile motion is a parabolic curve. The slope $\frac{ga}{2v^2}$ is found to be 0.000663

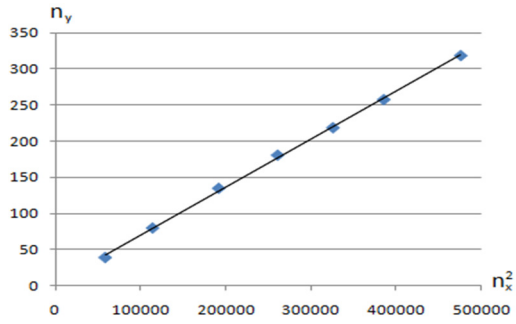

Fig 3. Line of best fit for $n_y \sim (n_x^2)$

The initial speed of the water flow v can be determined by measuring the time taken Δt for a small amount of water (volume V) to flow out the pipe with diameter d. The diameter of the pipe d can also be decided by using pixels coordinates

(so a vernier calipers is not needed) too. The speed is given by the equation

$$v = \frac{V}{\pi(d/2)^2}\frac{1}{\Delta t} \qquad (6)$$

The free fall acceleration can then be calculated. In our case the value is 9.3ms^{-2}, which is close to the know value 9.8ms^{-2}.

3. Summary

This is a quite interesting experiment or classroom demonstration. It doesn't need any special measurement apparatus such as vernier and it's very easy to perform. The students were also encouraged to do it at home. The experiment can help students get an intuitive understanding of horizontal projection and inspire students to work out convenient methods to solve problems. The idea of using digital camera and PC to measure distance can also be applied to other similar experiments.

Reference

[1] V. J. Ostdiek, D. J. Bord, *Inquiry into Physics,* 6th ed. (Thomson Brooks, Belmont, 2008), p. 62.

[2] W. Winn, *Introduction to Understandable Physics***,** (Authorhouse, Bloomington, 2010), V1, p. 3-16.

BASICS OF RENORMALISATION GROUP-DIVIDE AND CONQUER

M Sivakumar
*School of Physics, University of Hyderabad, Hyderabad - 500 046 (India)**

A first introduction to basic features of renormalisation group applied to critical phenomena is presented. As an illustration, 1D Ising model and Gaussian model are considered .Understanding of universality and scheme to compute critical exponents are also given.

I INTRODUCTION

Developments in Science owes itself to a miracle: miracle being phenomena in different length scales decouple.Without this feature, science would not have even taken off.

Let us understand this statement by taking fluids as illustration. Fluids have properties like viscosity, surface tension, and all of these features of fluids have been well studied. Now consider the description of fluids at different length scales. At $1m$ distance, description is as a continuous medium in terms of density and velocity and obeying Euler equations. At $10^{-5}m$ description will be as granular material.At $10^{-10}m$ it is described by atoms/molecules following quantum mechanics.At 10^{-15} description is in terms of nucleus applying strong interaction physics.At still smaller distance of $10^{-34}m$, laws of still unknown quantum gravity effects will show up.

Fortunately to study fluids at $1m$ scale we do not have to know,the still to be discovered quantum gravity laws at $10^{-34}m$.If that were so, even Newton might have to wait for quantum gravity to be solved ,to understand basic properties of matter.This is the miracle alluded to above: phenomena at different scales decouple, and each can be studied independently.Physics at each short distance scale only contributes to the values of the parameters in the succeeding larger scale.If those parameters are taken from experiments, then they can be studied independently. In the example above, strong interaction effects provide nuclear parameters, atomic physics provide atomic and molecular parameters.The molecular parameters provide macroscopic parameters of properties of matter like viscosity.

Difficulty arises when different length scales do not decouple.This happens close to critical point in continuous (or second order)phase transition.[1]In this transition order parameter increases from zero at T_c *continuously* to its maximum value at $T = 0$ as temperature is reduced.Recall that near T_C there are fluctuations in the order parameters in length scale given by correlation length ξ.Correlation length is the *maximum* distance to which spins are correlated.This means that fluctuations in the order parameter are from distance 0 to ξ.At T_C, since the correlation length diverges, the fluctuations are from 0 to all the way up to infinity.The degrees of freedom at different fluctuation length scale are entangled.Thus degree of freedoms associated with all length scales have to be taken into account.

This feature is also seen well in fluid system at criticality. The order parameter in this case is the density difference between liquid and vapour.Near T_c the fluctuations of all length scale shows up by the presence of liquid drops and vapor bubbles of varying sizes, all mingled within each other.Fluid has not made up its mind whether to condense or not.This density fluctuations is experimentally seen in scattering of light.When the fluid is scattered by light,it looses its transparent nature and there will be a white milkish patch ,due to scattering of wavelengths of order few thousand Angstrom. Since this is much larger than lattice spacing, lattice cannot be the cause.It happens only at critical temperature.Hence the large fluctuations are the culprits causing it. This is known as critical opalescence. Mathematically this is due to divergence in the density-density correlation function, equivalently compressibility, at critical point.

Similar feature also occurs in quantum field theory.Virtual particles of arbitrary energy scales are emitted and absorbed owing to uncertanity principle.There is fluctuation in energy in all scales contributing to the loop diagram.

The problems of these kind needs renormalisation group (RG) method to handle.This procedure, to handle these kinds of problem was developed by K.G.Wilson, who was awarded the Nobel prize for this contribution[2]. The method is to systematically eliminate the degree of freedoms at short distances and obtain effective theory for long distance.This will, as we will see, provide relation between parameters of theory at one length scale to another scale. More broadly speaking , Wilson scheme provides long distance effective description, wherein, short distance effects have been taken care of by suitable redefinition of the parameters valid for long distance.

How is this problem avoided in most of the system?For most of the systems, the correlation length is only a small number and whole system is superposition of small systems with very small correlation length. Since the de-

grees of freedom within the correlation length is small , approximation methods works.

In the following ,first we illustrate the RG procedure for 1d Ising model, followed by Gaussian model(defined below).Then the general procedure of RG will be abstracted, explaining Scaling and Universality. Finally we conclude how RG has given a new vantage point to understand quantum field theory.Some earlier reviews on RG are [3,4,5]. There are several excellent books on Renormalisation group and critical phenomena.A few recent ones include,[6,7]

II REAL SPACE RG OF 1D ISING MODEL

The 1D Ising model is defined by the Hamiltonian

$$H = -J\sum_i s_i s_{i+1} + \frac{H}{2}(s_i + s_{i+1}) \tag{1}$$

whose partition function is

$$Z = \sum_{s_1}\sum_{s_2}..\prod_i \exp ks_i s_{i+1} - \frac{h}{2}(s_i + s_{i+1}) \tag{2}$$

where $k = \beta J, h = H\beta$ The above equation(2) can be written as

$$Z = \sum_{s_i}\prod_i K(s_i, s_{i+1}) \tag{3}$$

where$K(s_i, s_{i+1}) = \exp(ks_i s_{i+1} - \frac{h}{2}(s_i + s_{i+1}))$ Note the parameters of the model are temperature T, Magnetic field H. Instead of summing over spins at all sites at one go, the spirit of RG is to first sum spin degrees at all even sites only.[8]

$$\sum_{s_2=\pm} K(s_1, s_2)K(s_2, s_3) \tag{4}$$

The above will be a function only of s_1, s_3. It is

$$\begin{aligned} &= \exp\{k(s_1 + s_3) - (h/2)(s_1 + s_3 + 2)\} \\ &+ \exp\{-k(s_1 + s_3) - (h/2)(s_1 + s_3 - 2) \equiv \tilde{K}(s_1) \end{aligned} \tag{5}$$

The other even sites elimination by summing over it will also have similar structure. Next we demand that equation(3) to have the same structure as the original Ising model but for a different set of parameters k', h'.

$$K(s_1.s_3) = \exp k'(s_1 s_3) - h'/2(s_1 + s_3) \tag{6}$$

Similar structure follows for all other even site spins. Next we get an explicit relation between old parameters (before even site spins were eliminated) and new ones (after they eliminated). $\tilde{K}(s_1, s_3)$ is a $2X2$ symmetric matrix with s_1, s_3 taking $\pm$ value.

$$\tilde{K}(+1,+1) = \exp(2k - 2h) + \exp -2k \tag{7}$$
$$\tilde{K}(+1,-1) = K(-1,+1) = \exp -h + \exp h \tag{8}$$
$$\tilde{K}(-1,-1) = \exp(-2k) + \exp(2k + 2h) \tag{9}$$

Similarly matrix elements of the symmetric $2X2$ matrix equation(6) are

$$K(+1,+1) = \exp(k' - h') \tag{10}$$
$$K(+1,-1) = \exp -k' \tag{11}$$
$$K(-1,-1) = \exp(k' + h') \tag{12}$$

By equating equations(7) and (10) we get the relation between primed parameters and unprimed ones:

$$\begin{aligned} \exp(-2h') &= \exp(-2h)\frac{cosh(2k - h)}{cosh(2k + h)} \\ \exp(4k') &= \frac{cosh(2k - h)cosh(2k + h)}{cosh^2 h} \end{aligned} \tag{13}$$

Thus there is a reduction of degrees of freedom(elimination of $N/2$ even spins) and concomitant change in parameters.

The second step is to rescale the distance in units of lattice spacings to bring it back to the original system.With even site spins eliminated the lattice spacing between the remaining spins is *twice* the original spacing.To compare with the original system , we must rescale the distance by *half* so that the lattice spacing is the same.Though in general scaling may require scaling spin degrees also , in this example there is no necessity for it. This process can be repeated with parameters changing under each iteration. Next we find the fixed point of the transformation.

It is convenient to define $x = \exp(-4k)$ and $y = \exp(2h)$ then equation(13) is

$$\begin{aligned} x' &= f(x,y) = x\frac{(1+y)^2}{(1+yx)(y+x)} \\ y' &= g(x,y) = y\frac{x+y}{1+xy} \end{aligned} \tag{14}$$

These equations provide the recurrence relations between the parameters. Next we have to identify the fixed point of the transformation.These are the solutions of the equation :$x' = x, y' = y$ i.e,

$$\begin{aligned} x &= x\frac{(1+y)^2}{(1+yx)(y+x)} \\ y &= y\frac{x+y}{1+xy} \end{aligned} \tag{15}$$

The solutions are

1.
$$x = 1, y \tag{16}$$
which is $T \to \infty$, describing paramagnetic phase and has zero correlation length and hence not a critical point.

2.
$$x = 0, y = 1 \tag{17}$$
This is $T = 0, H = 0$, which is a critical point and has infinite correlation length.This critical fixed point is what we will be interested in.

We will study the behavior of the fixed point of critical point.Taylor expand the recurrence relation equation (14)around critical fixed point $x^\star = 0, y^\star = 1$.

$$x' = x^\star + \frac{\partial f}{\partial x}\delta x + \frac{\partial f}{\partial y}\delta y \tag{18}$$
$$y' = y^\star + \frac{\partial g}{\partial x}\delta x + \frac{\partial g}{\partial y}\delta y \tag{19}$$

Where $\delta x = x - x^\star$ and $\delta y = y^\star - y$, similarly for $\delta x'$ and $\delta y'$. This gives using equation(15)

$$\delta x' = 4\delta x \tag{20}$$
$$\delta y' = 2\delta y \tag{21}$$

This gives the deviation from fixed point after each iteration.Since ,by summing over all even sites spins, we have effectively increased the distance by 2 the above is actually

$$\delta x' = 2^2\delta x \tag{22}$$
$$\delta y' = 2\delta y \tag{23}$$

In general if b units were scaled for a variable A,then we have $\delta A' = b^{l_A}\delta A$

For Ising model this gives $l_t = 2$ and $l_h = 1$.As we shall see this can be used to calculate the critical exponents.

As the RG transformations were done on spins on a lattice sites in 1d coordinate space, this is real space RG. Next we consider RG in momentum space as opposed to real space.

III MOMENTUM SPACE RG OF GAUSSIAN MODEL

Gaussian model is defined by the Hamiltonian

$$\beta H = \int d^d x \frac{1}{2}[\bigtriangledown\phi.\bigtriangledown\phi + r_0\phi.\phi] \tag{24}$$

Note the fields appear quadratically in the Hamiltonian, hence the name Gaussian.[5] In momentum space ,this Hamiltonian is

$$\beta H = \frac{1}{2}\int \frac{d^d k}{[2\pi]^d}(k^2 + r_0)\phi(k)\phi(k)^* \tag{25}$$

$$Z = \int \prod_k d\phi(k)\exp(-\beta H) \qquad where \;\; 0 < k < \Lambda \tag{26}$$

Divide k into two regions $0 < k < \Lambda/s$ and $\Lambda/s < \Lambda$ Note this is a sharp division of wave vectors into two divisions. Divide the field $\phi(k) = \phi'(k) + \sigma(k)$ where
$\phi(k) = \phi'(k) \quad 0 < k < \Lambda/s$
$\phi'(k) = 0 \qquad \Lambda/s < k < \Lambda$
$\sigma(k) = 0 \quad 0 < k < \Lambda/s$
$\phi(k) = \sigma(k) \quad \Lambda/s < k < \Lambda$
Also $\int dk\phi'(k)\sigma(k) = 0$ since there is no overlap in non vanishing region .Define $\bar{dk} = \frac{d^d k}{(2\pi)^d}$

$$\beta H = \frac{1}{2}\int \bar{dk}|\phi' + \sigma|^2(k^2 + r_0) \tag{27}$$
$$= \frac{1}{2}\int \bar{dk}(\phi'\phi' + \sigma\sigma)(k^2 + r_0) \tag{28}$$
$$Z = \int d\phi' e^{-\int \bar{dk}\frac{1}{2}(k^2+r_0)|\phi'|^2}\int d\sigma e^{-\int \bar{dk}\frac{1}{2}(k^2+r_0)|\sigma(k)|^2} \tag{29}$$

Observe there is no interference between low and high wave vector modes and they factorize as we have only Gaussian model.If interaction like ϕ^4 is added, this feature will fail.

Denote by $Z_>(Z_<)$ contribution of $\sigma(k)(\phi')$ field. We are after the long wave vector modes.The contribution of $Z_>$ is only for the free energy and not for the recursion relation between parameter r_0 .Hence we can ignore them.

$$Z = Z_> \int \prod_{k=0}^{\Lambda/s} \exp - \int \bar{dk}\frac{1}{2}(k^2 + r_0)|\phi'|^2 \tag{30}$$

The next part of the recipe of RG is to rescale k such that it goes over to the same range i.e, between 0&Λ. k scales as $k \to sk$ so that rescaled k ranges from 0to Λ. The third part of RG is, ϕ' has to be scaled correspondingly so that the k^2 coefficient remains $\frac{1}{2}$.

$$\phi'(k) \to \phi(k) = (1/z)'\phi(k) \tag{31}$$

Scaling $k \to k' = sk$, we regain the same range for k' ie; $0 \to \Lambda$.This scales H to

$$\bar{d}'ks^{-d}(k'^2 s^{-2} + r_0)z^2\phi'('k) \tag{32}$$

Keeping the coefficient of kinetic energy term (without dimensional parameter) invariant gives

$$k'^2\phi' s^{-d-2}z^2 = k'^2\phi' \tag{33}$$
$$\text{gives} \quad z = s^{\frac{d}{2}+1} \tag{34}$$

$$r_0 \to r_0' = s^{-d}z^2 = s^{-d+d+2}r_0 = s^2 r_0 \equiv r(s) \tag{35}$$

This equation(35) relates the (only) parameter in the theory at different scales.For infinitismal change of momentum scale

$$\begin{aligned} r(s+ds) &= (s+ds)^2 r_0 \\ r(s) + \frac{dr}{ds}ds + .. &= s^2 r_0 + 2sr_0 ds + .. \\ \frac{dr(s)}{ds} &= 2sr_0 \\ s\frac{dr}{ds} &= 2s^2 r_0 \\ s\frac{dr}{ds} &= 2r(s) \\ \frac{dr}{d\ln s} &= 2r(s) \end{aligned}$$

This equation represents $'$flow $'$of the r_0 under RG transformation.

The fixed point of the transformation is solution of$\frac{dr}{d\ln s} = 0$.ie $r \equiv r^* = 0$ This fixed point is Gaussian fixed point.Once the RG transformation reaches this point , r will remain stay put-ie;fixed.

Two remarks are in order

1)In Gaussian model no new terms are generated under RG transformation. In this case it is similar to 1d Ising model. In general, new terms will be generated, with coefficients dependent on wave vectors too.

2)When we refer as coupling constant, the word constant makes us take them to be a universal number like Plancks constant or π.But thats not correct, as the extension 'constant' is a misnomer.It is more a coupling function , whose value depends on the length scale at which it is measured.The recursion relation provides the change in the value of the so called constant as we change the scale at which we observe.Electrons charge, as listed in tables, is related to the coupling constant at zero k .

IV GENERAL FEATURES

GENERAL FEATURES

The issues RG tries to explain include:a) Universality of critical exponents b)calculation scheme for calculating exponents.

Recipe for RG

Ingredients Required:

a)Hamiltonian with an order parameter (or field)

b) a method for introducing cut-off (there is no unique choice: for real space , it is lattice, for momentum space, it can be sharp cut-off, like theta function, or smooth cut-off

c) a scheme for taking degrees of freedom associated with short distances/large wave-vectors.If the scheme has a controlled approximation it is better.

Procedure:

Take the given Hamiltonian with the chosen cut-off method. Integrate the short distance degrees of freedom by applying the scheme chosen: this can be ,in real space by majority rule/avarage spin for the block spin, in k-space perturbatively integrate over the high momentum modes of the field. Let the momenta integrated by between $\Lambda > k > \Lambda/s$. The resulting Hamiltonian contains fields for modes of momenta of only $k < \Lambda/s$.But we cannot compare this with the starting system , as they are defined in reduced range of k-space.To bring them back to their original range, *scale* momentum /coordinate. This ,in general, needs *rescaling of field*, ie change in the magnitude of the field. The net result of these three operations is that the original Hamiltonian,with a given set of couplings, transforms to a Hamiltonian with different coupling constant and (in general)new set of couplings .This provides the relationship between the two set of parameters.Take the relationship between the original set of couplings and new set of couplings.

Serve it hot for consumption!

Classification of Scaling variables

Given an order parameter field and a symmetry , we can consider the most general Hamiltonian involving them consistent with the symmetry.Each term will have a coupling parameter.Note here though the coefficients are referred to as 'coupling constants', it is better to regard them as parameters in the theory.Define a Hamiltonian space , which is the space of coupling constants.If one wishes to call Hamiltonians with different couplings as different theories,then this space is a 'theory space'.For eg; scalar order parameter case,

$$H = |\bigtriangledown \phi|^2 + r\phi^2 + u\phi^4 + g_1\phi^6 + g_2|\bigtriangledown \phi|^2\phi^2 + ... \quad (36)$$

Thus in general it has infinite number of couplings.To make it better to handle, we will consider a subspace , which is m dimensional, with couplings $K_\alpha = \{K_1, K_2, ..K_m\}$.This set of values of K can be represented as a point in m−dimensional space. Under RG transformation, the set of couplings will change to another value, which can be pictured as a point in theory space moving to a different space.

$$K_\alpha \to K'_\alpha = R_\alpha(K_1, ..K_m) \quad (37)$$

Thus, by repeated RG transformation $K \to K' \to K''$.. The transformation is said to reach a *fixed point* if $K \to K^* \to K^*$. ie point in theory space stops moving further under RG flow.K^*_α are the couplings at the fixed point. The correlation length scales under RG transformation, since one of the action of RG is to scale the

distances/momenta. Correlation length in extrinsic unit like cm is invariant.But in units of intrinsic length scale changes.$\xi(K) \to \xi'(K')$.At fixed point,$\xi(K^*) \to \xi(K^*) = l^{(-d)}\xi(K^*)$. ξ under scaling must remain invariant.No finite number will be invariant.Only $0, \infty$ will remain so.Hence fixed point physics must correspond to these two values of ξ.The value 0 correspond to stable bulk phase as in that phase, degrees of freedom have only short range correlation.$\xi = \infty$ case represents the (unstable) critical phase.

Given the fixed point,the couplings are expanded about it.

$$K'_\alpha = R_\alpha(K) \quad (38)$$
$$K^*_\alpha + \delta K'_a = R_\alpha(K^* + \delta K) \quad (39)$$
$$= R_\alpha(K^*) + \frac{dR_\alpha}{dK_\beta}\delta K_\beta \quad (40)$$
$$= K^* + \frac{dR_\alpha}{dK_\beta}\delta K_\beta \quad (41)$$
$$\text{define} \quad \frac{dR_\alpha}{\delta K_\beta} \equiv M_{\alpha\beta}(l) \quad (42)$$
$$\delta K^* = M(l)\delta K \quad (43)$$

Note $M_{\alpha\beta}$ is $m \times m$ matrix and is not assured to be symmetric.Let $V^{(\sigma)}, l^\sigma(l)$ be the right eigenvector and corresponding eigen value.$\sigma = 1, ..m$.
Expanding $\dot{K}$ in terms of the eigenvectors

$$\delta K_\alpha = a^{(\sigma)}_{\alpha\beta} V^{(\sigma)}_\beta$$
$$\delta K'_\alpha = a'^{(\sigma)}_{\alpha\beta} V^{(\sigma)}_\beta \quad (44)$$
$$a'^{(\sigma)} = l^{(\sigma)}(l) a^{(\sigma)} \quad (45)$$

Now what can we say about l^σ,eigenvalues of M? The RG transformation obeys three axioms of group: a) existence of identity-$l = 1$ gives $M = I$
b)Existence of product rule .If represents Matrices associated with integrating momentas $\Lambda \to \Lambda/l_1 \to \Lambda/l_2$which can be achieved directly $\Lambda \to \Lambda/(l_1 l_2)$. Hence $M(l_1)M(l_2) = M(l_1 l_2)$
c)Ofcourse associativity is satisfied as it is a matrix. Importantly inverse does *not* exist.Once we trace out some degrees of freedom , we cannot uniquely fix the original configuration.This is like given a matrix we can tell its trace, but if I give you trace of a matrix, can you tell me a unique matrix which has this trace?

Hence the transformation does not form a group in the precise sense.It is sometimes referred to as semi-group.

These three properties of the group restricts the eigenvalue $l^\sigma(l) = l^{d_\sigma}$ The eigenvalue is given by d_σ. The eigenvector V^σ is called **Relevent** if the associated eigenvalue $d_\sigma > 0$, **Irrelevant** if $d_s < 0$, **Margininal** if $d_\sigma = 0$ Why are they called so?By repeated RG transformation , for relevent eigenvector its contribution to couplings K_α will go on increasing as $d_\sigma > 0$.Hence they are relavent. Similarly contribution of irrelevent eigenvectors will be decreasing.Hence it is irrelevent. Marginal variable does not contribute at linear order and hence to look at it contribution one should go beyond linear order.
Let $K_1, K_2..K_n (n < m)$ be the couplings which are relevant and the remaining irrelevant. For simplicity we consider there is no marginal variable. This classification of relevant,irrelevant and marginal will turn out to be important to understand universality and calculation of exponents.These definitions are with respect to a fixed point.The same variable with respect to a different fixed point can change their relevancy.

Universality

1. To understand, how systems with different T_C and different microscopics share the same exponents near criticality.

2. Definition:*critical surface* : In the m dimensional theory space, critical surface is a subspace, defined by setting all relevent couplings to zero.This is like in 3d space we can define a 2d surface,xy plane, by setting $z = 0$.The main feature of the Critical surface is the fixed point is contained in it. Since relevant parameters are zero and the effect of irrelevant ones will die down ,any point on the critical surface will flow under RG to the fixed point.This is the importance of the critical surface. The dimension of the critical surface is $m - n$.The number of conditions required to define this critical surface is known as co-dimension, which is n here.In the case of magnetic system, we will see that the relevant variables are temperature and the magnetic field, and hence the codimension of the critical surface is two.

3. On the theory space we are going to define two kinds of transformation: one a physical transformation ,which can be done in principle by a "knob"in experiment.This transformation will bring the system to its critical point. The second is a mathematical RG transformation, which cannot be achieved by experimentalists by tuning "knobs" of apparatus, but it exits only as theorists construction.

4. Consider a line piercing the critical surface at a point P.This change is effected by physical transformation, and the system is tuned to be at the point P .For eg in magnetic system this physical transformation is achieved by tuning the system to be at its $T = T_C \quad H = 0$ .Similarly a different system will be piercing the critical

surface at a different point Q. The critical surface contains fixed point.Hence both the points P, Q which are on the critical surface, and are at their respective critical point, under RG flow to the fixed point.(fig-1)
What happens if the system is slightly off the critical surface? This is done by the physical transformation by tuning the system close to the critical point. Under RG transformation this point p' will flow close to the fixed point.Since the system is not exactly on critical surface, the relevant variable is not exactly zero, but close to it.Near the fixed point , due to their relevance , RG effects amplify their effect, and the trajectory moves away from the fixed point.Similar behavior is expected for the system Q' which represent the system Q slightly away from the critical point. For eg; these two points can represent elements Ni and iron.(fig-2) In fact for all points slightly off the critical surface will undergo similar behavior.

This explains that all points on the critical surface will have universal behavior as their long distance effective description will be governed by the same fixed point.The critical exponents are provided by the eigenvalues of *relevant* variable of this fixed point. This has been seen in earlier examples.
To summarise: all systems on the critical surface,ie Hamiltonians having these $m - n$ irrelevant couplings will all share the same exponents and have the same long distance behavior.The microscopic parameters which distinguish the different systems sharing the same universal class, are irrelevant in the RG sense, explaining universality. It explains the universality by staying close to T_C , it is the long distance "cooperative behavior" and not short distance dirty details that are dominating.

SCALING

1. At criticality there are fluctuations of order parameter at all length scales.Hence there is no specific length scale which shows up. To whatever length scale we zoom in the system will appear the same. The scale invariance shows up in this way.

2. Mathematically it shows up in correlation function $G(\mathbf{x}, \mathbf{y})$. Correlation function must be decreasing function of the distance between the points.It can be exponentially falling or power law dependance. But exponential functions are not scale invariant.

$$\exp(\lambda x) \neq \lambda \exp(x) \tag{46}$$

But power law functions have this property.

$$\frac{1}{(\lambda x)^p} = \lambda^{-p} \frac{1}{x^p} \tag{47}$$

This means there is self-similarity as the distances are scaled. Correlation function at *criticality* is a power law function.Mathematically ,this is seen as

$$G(\mathbf{x}, \mathbf{y}) \sim \frac{\mathbf{1}}{|\mathbf{x} - \mathbf{y}|^{\mathbf{d-2}+\eta}} \tag{48}$$

Here η is a critical exponent which characterizes the power law behavior. It is zero for Gaussian model as different modes of the field decouple. When it is non-zero, a)it shows how fluctuation at lattice level(or at momentum cut-off)gets coupled with long distance fluctuation and b)it reflects in failure of naive dimensional analysis of fields .Fields then have dimensions different from the engineering dimension;they get "anomalous dimension". Physically the power law behavior is seen as the presence of clusters of up and down spins of all sizes or in fluid system as drops of liquid and bubbles of gas of all sizes. This behavior is also similar to the structure of some naturally occurring objects like: clouds, river basin,..There is self similarity of structure at all length scales.These are known as fractal structure.
Thus there is a deep connection between scale invariance-power law behavior-criticality.

3. Singular part of free energy close to criticality has scaling form.This follows from RG point of view.Consider ,1d Ising model as illustration. Free energy per unit site (which, incidentally is an intensive quantity)is $f \propto \frac{1}{N} \ln Z_N$
Under RG first note that $Z_N(K)$ is invariant, where K denote couplings. Let us split the N degrees of freedoms into N' and N''. Out of N sites N' has been first traced.

$$f(K) = \frac{1}{N} \ln[Tr_N e^{-H(K)}] \tag{49}$$

$$= \frac{1}{N} \cdot \frac{N'}{N'} \ln Z_{N'}(K') = \frac{N'}{N} f(K') \tag{50}$$

$$\text{Since} \quad \frac{N'}{N} = b^{-d}. \tag{51}$$

$$\tag{52}$$

Thus f has the required scaling behavior.After b^d degrees of freedoms have been summed out ,$K \to K_b$, where K_b is given in terms of K by RG equation.

$$f(K) = b^{-d} f(K_b) \tag{53}$$

For specific case of couplings being temperature$t$and magnetic field h, (which are relevant parameters in Ising model)

$$f(t,h) = (b^{-d})^l f(t_l, h_l) \tag{54}$$

calculation of exponents

1. Recall that from the linear analysis of the RG transformation for parameter, say K, about the fixed point , we got $K_b = b^{y_K}$. Hence $t_b = b^{y_t}, h_b = b^{y_h}$.The quantities y_t, y_h are calculable from RG transformation and are > 0 as they are relevant . We will see that the exponents are given in terms of them ,using scaling form of free energy.

   From the scaling form of the free energy

$$\begin{aligned} f(t,h) &= b^{-d} f(b^{y_t}t, b^{y_h}h) \\ \text{Choose } b \text{ such that} \quad b &= t^{-1/y_t} \\ f(t,h) &= t^{d/y_t}\Phi(t^{-y_h/y_t}h) \end{aligned} \tag{55}$$

   As illustration few of critical exponents are calculated below:

2. Exponent β.

$$\begin{aligned} m(t,h) \equiv \frac{\partial f}{\partial h} &= t^{d/y_t}\Phi' \quad t^{-y_h/y_t} \\ m(t,0) &\sim t^{d/y_t - y_h/y_t} \\ \beta = \frac{d-y_h}{y_t} & \end{aligned} \tag{56}$$

3. Exponent γ

$$\begin{aligned} \chi &\equiv \frac{\partial m}{\partial h} \\ &= t^{\frac{d-y_h}{y_t}}\Phi'' \quad t^{-y_h/y_t} \\ \chi(t,0) &\sim t^{\frac{d-2y_h}{y_t}} \\ \gamma &= \frac{d-2y_h}{y_t} \end{aligned} \tag{57}$$

4. Exponent δ
   Exponent $\delta$is defined by $M \sim h^{1/\delta}$ at $t = 0$. consider

$$\begin{aligned} M &= \frac{\partial f}{\partial h} \\ &= t^{d/y_t}\Phi' \quad t^{-y_h/y_t}. \end{aligned} \tag{58}$$

   We cannot put $t = 0, h \neq 0$ in the above as M itself vanishes,which is not correct.As $x \to 0 \quad \Phi'(x) \to x^q$ with q to be determined such that M is finite. As $t \to 0$

$$\begin{aligned} M &= t^{(d-y_h)/y_t}\left(\frac{h^q}{t^{qy_h/y_t}}\right) \\ &= t^{(d-y_h)/y_t - qy_h/y_t} h^q \end{aligned} \tag{59}$$

$$\begin{aligned} \text{demanding power of } t = 0 \quad q &= \frac{d-y_h}{y_h} \\ \text{hence} \quad \delta^{-1} &= \frac{d-y_h}{y_h} \end{aligned} \tag{60}$$

Conclusion

RG is a framework to understand the long distance behavior of a system.The theory valid at long distance is obtained by systematically eliminating the short distance effects and incorporating them as change in the parameters defining the theory. Thus the seemingly insurmountable difficult problem of all length scales coupled,is won by diving into smallest length scale and conquering them one by one: *divide and conquer* is the policy! .
RG has also shed light on quantum field theory.In the olden days ,in quantum field theory,'good'(ie renormalisable) theories were expected to be valid for all length scales upto zero diatance.A cut-off was introduced more as a convenient intermediary to absorb certain infinities. But RG has provided a vantage point to understand some of the behavior.Now cut-off is considered as a necessity, above which the theory is not defined. Some times it is possible to lump the effects of short distances as change in finite number of parameters.They are, in older language 'good' theories.In such theories their region of validity will be decided by experiments.Sometimes it is not possible and it may require infinite number of parameters.These were considered earlier as "bad" (non-renormalizable)theories. But even these theories can have a predictive power to an arbitrary level of accuracy.This insensitiveness of the long distance phenomena to short distance behavior (which is is universality in critical phenomena) is presently seen as renormalisablity feature in quantum field theory.
RG is a broad framework and it can be considered as giving a theory of writing theories.Its application to more areas ,one can say,is in beginning stages.

Acknowledgment

I thank Sudharsana.V and K.Sravan Kumar for help in preparing the manuscript and H.S.Sharatchandra and Siddhartha Sen for encouragement.

References

[1] Introduction to phase transitions and critical Phenomena-Stanley H.E(Oxford,1971)

[2] The renormalization group and critical phenomena-Kenneth G. Wilson Rev. Mod. Phys. 55, 583 (1983),

[3] Teaching the renormalization group-Humphrey J. Maris and Leo P. Kadanoff Am. J. Phys. 46, 652 (1978),

[4] Renormalization-group approach to interacting fermions -R. Shankar,Rev. Mod. Phys. 66, 129 (1994)

[5] Critical Phenomena: An Introduction from a modern perspective-Somendra M. Bhattacharjee -cond-mat-0011011

[6] Lectures on phase transitions and renormalisation group(Addison-Wesley, Reading, Ma, 1992)by N.Goldenfeld,

[7] Quantum field theory and critical phenomena-(Clarendon Press; Fourth Edition edition 2002) By J.Zinn-Justin,

[8] Soluble Renormalization Groups and Scaling Fields for Low Dimensional Ising Systems- D.R. Nelson, M.E. Fisher, Annals Phys.91:226-274,1975.

---

* mssp@uohyd.ernet.in

Demonstration of Interference of Polarized Light with a Wedge Depolarizer

Shengli Pu
College of Science, University of Shanghai for Science and Technology, Shanghai 200093, China
Email: shlpu@usst.edu.cn
(*Submitted* June 2010)

Abstract

A simple experimental configuration for the demonstration of interference of polarized light is presented in this paper. Using the wedge depolarizer, a nice and direct demonstration of interference of polarized light is realized, which would help to impress on students the phenomena of interference of polarized light intuitively. Moreover, this experiment can be easily implemented in the undergraduate/postgraduate optics laboratory because of its simple setup, and there is no need for expensive equipment.

1. Introduction

For some applications, the polarization-sensitive devices may cause considerable errors or degrade the performance of the systems when the incident light is not completely unpolarized. For example, the polarization-sensitive detector will result in errors and noise in the optical sensing and spectrum measurement systems; the polarization-dependent effects in optical fiber communication system may reduce its performance. Therefore, completely unpolarized light is desirable for some cases. Under this requirement, the term depolarization and the corresponding device depolarizer (which couple the polarized light into the unpolarized one) occur. As we know, it is easy to get the polarized light via unpolarized one (e.g. using a polarizer). Contrarily, it is more or less difficult to depolarize the polarized light. Thanks to the development of depolarizers, the equivalently unpolarized light can be realized at present. Besides these, I have casually found that the commercially available wedge-type depolarizer can be employed to demonstrate the interference of polarized light easily and nicely in our optics laboratory. The underlying physical principle is fundamental for undergraduate/postgraduate students, but the interference patterns are splendid, which may be impressive for students. This article first gives a brief introduction to the present depolarizers and the theory of interference of polarized light. Then the wedge depolarizer is chosen to demonstrate the interference of polarized light. With the wedge depolarizer, versatile and obvious interference patterns are observed experimentally.

2. Depolarizers and interference of polarized light

Strictly speaking, the present depolarizers in fact are wavelength-dependent[1,2] or temporal[3]/spatial[4] pseudo-depolarizers according to the mechanisms of depolarization. The transmitted light of the currently used depolarizers are not genuine unpolarized light, but compose of much light with various wavelength-dependent states of polarization or various states of polarization temporally/spatially. The collective effects of the transmitted light equal those of the unpolarized light. So the current depolarizers are pseudo-depolarizers in nature. According to their structures, the typical pseudodepolarizers can be classified into two kinds: Lyot depolarizers and wedge depolarizers. The Lyot depolarizer consists of two crystalline plates of thickness ratio 2:1,

whose optical axes lie in the planes of the plates and are oriented at 45° to one another.[5,6] It creates various degrees of elliptical polarization as a function of wavelength, therefore it is a wavelength-dependent depolarizer and not suitable for the monochromatic light application. The wedge depolarizer consists of a wedge birefringent crystal, whose optical axis lies in the plane of the wedge and usually at 45° to the input polarization for the maximum performance of depolarization. Consequently, it is sensitive to the input polarization direction. Fig. 1 schematically draws the structure of the wedge depolarizer. Because of the varying thickness of crystal at different loci of the wedge, the phase retardation between the ordinary and extraordinary light (depending on the thickness) is diversified. This results in the transmitted light composed of multiple degrees of elliptical polarization.

The typical experimental setup for investigating the interference of polarized light is shown in Fig. 2. A linearly polarized incident light impinges on the retardation sheet, and then passes through an analyzer. The interference of polarized light can be observed on the screen. If the intensity of the linearly polarized incident light is I_0, the intensity of the transmitted light on the screen is given as follows (according to Malus's law),

$$I = I_0(\cos^2\alpha\cos^2\beta + \sin^2\alpha\sin^2\beta + 2\cos\alpha\cos\beta\sin\alpha\sin\beta\cos\delta)$$

$$= I_0\cos^2(\alpha+\beta) + \frac{I_0}{2}\sin 2\alpha\sin 2\beta(1+\cos\delta), \quad (1)$$

where α / β are the included angles between the transmission axes of the polarizer/analyzer and the electric vector of the extraordinary (or ordinary) light in the retardation sheet (see Fig. 2), δ is the phase retardation of the transmitted light, which depends on the relative orientation of the linearly polarized light and the parameters of the retardation sheet (also depends on wavelength for polychromatic light). By changing α, β or δ, the intensity or patterns on the screen can be changed according to Eq. (1). This will demonstrate the interference of polarized light.

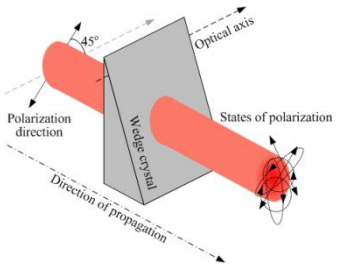

Figure 1. Schematic structure of the wedge depolarizer.

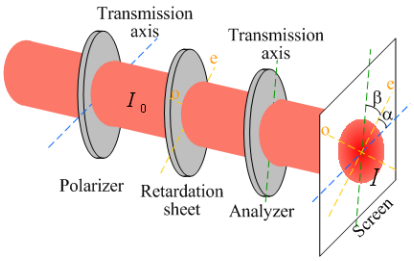

Figure 2. Experimental setup for investigating the interference of polarized light.

3. Experiment

As the wedge depolarizer is a birefringent crystal with varying thickness and commercially available, it is a good candidate device for demonstrating the interference of polarized light. When the retardation sheet in Fig. 2 is replaced with a wedge depolarizer, wonderful interference patterns of the polarized light can be observed. From Eq. (1), the following results are easily obtained and the corresponding experimental

interference patterns are photographed by a digital CCD camera and shown in Figs. 3-6, respectively. The spatial configurations of the optical components are schematically depicted in the right panels of the corresponding figures.

When α =0° and β =90° (or α =90° and β =0°), I =0, viz dark field happens on the screen, which can be seen in Fig. 3.

When α =0° (or 90°), $I = I_0 \cos^2 \beta$ (or $I_0 \sin^2 \beta$), namely the intensity on the screen are uniform spatially and only depend on the value of β [see Figs. 4(a) and (b) for β =30° and 45°, respectively]. From Fig. 4, the intensities of the interference patterns are almost uniform everywhere. The brightness in Fig. 4(b) is slightly weaker than that in Fig. 4(a), which is due to $\cos^2 45^o < \cos^2 30^o$.

When β =0° (or 90°), $I = I_0 \cos^2 \alpha$ (or $I_0 \sin^2 \alpha$). This is very similar to Case 2 (Fig. 4) and the experimental interference patterns are not shown here in.

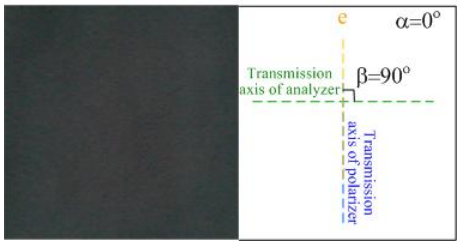

Figure 3. Interference pattern for α =0° and β =90°. Dark field happens on the screen.

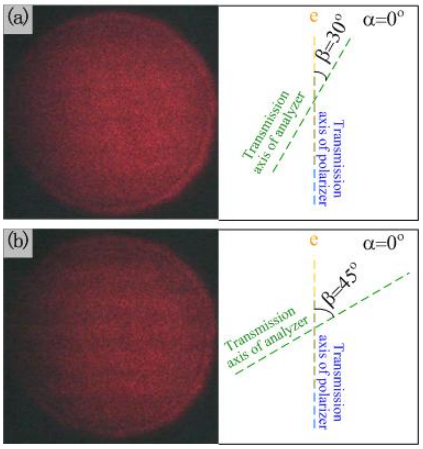

Figure4. Interference patterns for α =0°, (a) β =30° and (b) β =45°. Intensities of the interference patterns are almost uniform spatially.

For the above cases, the second term on the right hand side of Eq. (1) is always equal to zero. On the other hand, it will have various values when $\alpha \neq 0^o/90^o$ and $\beta \neq 0^o/90^o$. For the fixed values of α and β, the intensity on the screen only depends on the phase retardation δ, i.e. the thickness of the retardation sheet (considering monochromatic light). As the wedge depolarizer has a varying thickness spatially, the spatial distribution of the intensity on the screen I must be periodic like the variation of the thickness of the depolarizer. This periodic distribution of intensity constitutes the interference fringes and their orientation coincides with the direction of the arris of the wedge depolarizer (viz the isopachous lines of the wedge). Under this situation, the first term on the right hand side of Eq. (1) influences the visibility of the fringe patterns. And then the phenomena of the interference can be classified into two cases (maintaining $\alpha \neq 0^o/90^o$ and $\beta \neq 0^o/90^o$).

When $\alpha + \beta$ =90° (or 270°), the intensity of the dark regions of the interference fringe patterns equals zero [because the first term on the right hand side of Eq. (1) equals zero], which results in

the maximum visibility of the fringe patterns. (a) Maximum intensity of the bright fringe happens for $\alpha = \beta = 45^o$ [see Fig. 5(a)]. (b) Reduced intensity of the bright fringe happens for other values of α and β, for instance, $\alpha = 30^o$ and $\beta = 60^o$ [see Fig. 5(b)]. From Fig. 5, it is revealed that there is almost no light in the dark areas of the interference patterns. Comparing with that in Fig. 5(a) ($\alpha = \beta = 45^o$), the reduced intensity of the bright fringe in Fig. 5(b) ($\alpha = 30^o$ and $\beta = 60^o$) is not obvious, but can be noticed by careful observation of the two photographs.

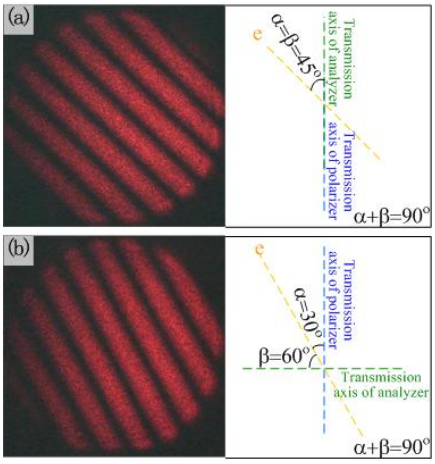

Figure 5. Interference patterns for (a) $\alpha = \beta = 45^o$ and (b) $\alpha = 30^o$, $\beta = 60^o$ ($\alpha + \beta = 90^o$ for both situations). Maximum visibility of the fringe patterns happens.

When $\alpha + \beta \neq 90^o$ (or 270^o), the visibility of the patterns will be degraded contributed to the nonzero value of the first term on the right hand side of Eq. (1). Figs. 6(a) and (b) display the experimental interference patterns for $\alpha = \beta = 30^o$ and $\alpha = 30^o$ and $\beta = 45^o$, respectively. It is apparent that the intensity of the dark regions of the interference patterns is nonzero, which is different from Fig. 5. Consequently, the visibility of the interference patterns weaken to some extent compared with those in Fig. 5.

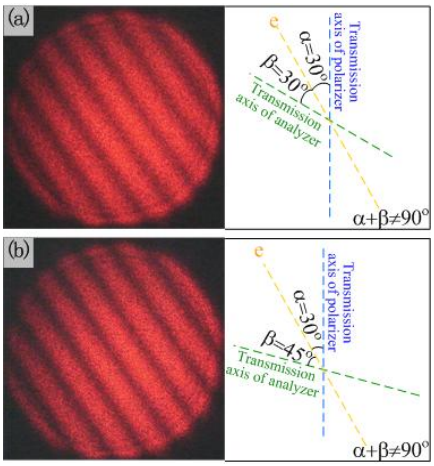

Figure 6. Interference patterns for (a) $\alpha = \beta = 30^o$ and (b) $\alpha = 30^o$, $\beta = 45^o$ ($\alpha + \beta \neq 90^o$ for both situations). The visibility of the fringe patterns is degraded relatively.

Figs. 5 and 6 show that the orientation of the interference fringes always coincides with the optical axis of the wedge depolarizer and is independent of the positions of the transmission axes of the polarizer and analyzer. This confirms the forementioned theoretical analysis. Further experiments have readily found that the orientation of the interference fringes can be changed by rotating the wedge depolarizer about the propagation direction of the light beam, i.e. its optical axis. In short, the above experimental results have a good agreement with the theoretical predictions based on Eq. (1).

4. Conclusions

Experiments indicate that the commercially available wedge depolarizer is a useful tool for the easy and impressive demonstration of the interference of polarized light. It may help students better understand the nature of polarized

light. In addition, the method presented in this paper is cost-effective to equip the corresponding undergraduate/postgraduate optics laboratory with wedge depolarizers to investigate the interference of polarized light.

Acknowlegements

This work was funded by the Research Fund for Selecting and Training Excellent Young Teachers in Universities of Shanghai, Shanghai Municipal Education Commission; and partially supported by the National Natural Science Foundation of China under Grant No. 10704048. The author thanks Professor J. Shen in our department for his enlightening discussions.

References :

1. S.-L Lu, and A. P. Loeber, J. Opt. Soc. Am. **65**, 248 (1975).
2. A. A. Kokhanovsky, Am. J. Phys. **72**, 258 (2004).
3. I. Yoon, B. Lee, and S.-J. Park, J. Lightwave Technol. **25**, 1848 (2007).
4. D. Zhang *et al.*, Opt. Eng. **46**, 070504 (2007).
5. A. P. Loeber, J. Opt. Soc. Am. **72**, 650 (1982).
6. P. H. Richter, J. Opt. Soc. Am. **69**, 460 (1979)